

Accelerated Dilution of Liquefied
Natural Gas Plumes with Fences and Vortex Generators

FINAL REPORT
(August 1981 - May 1982)

prepared by

K. M. Kothari and R. N. Meroney

Fluid Mechanics and Wind Engineering Program
Department of Civil Engineering
Colorado State University
Fort Collins, Colorado 80523

CER81-82KMK-RNM79

for

GAS RESEARCH INSTITUTE

Contract No. 5014-352-0203

GRI Project Manager

Steve J. Wiersma

Environment and Safety Department

May 1982



U18401 0076508

Engineering Science

FEB 3 1983

Branch Library

GRI DISCLAIMER

LEGAL NOTICE This report was prepared by Colorado State University as an account of work sponsored by the Gas Research Institute (GRI). Neither GRI, members of GRI, nor any person acting on behalf of either:

- a. Makes any warranty or representation, expressed or implied with respect to the accuracy, completeness, or usefulness of the information contained in this report, or that the use of any information, apparatus, method or process disclosed in this report may not infringe privately owned rights; or
- b. Assumes any liability with respect to the use of, or for damages resulting from the use of, any information, apparatus, method, or process disclosed in this report.

REPORT DOCUMENTATION PAGE		1. REPORT NO. GRI-81/0074	2.	3. Recipient's Accession No.
4. Title and Subtitle ACCELERATED DILUTION OF LIQUEFIED NATURAL GAS PLUMES WITH FENCES AND VORTEX GENERATORS			5. Report Date May 1982	
7. Author(s) K. M. Kothari and R. N. Meroney			6.	
9. Performing Organization Name and Address Civil Engineering Department Colorado State University Fort Collins, Colorado 80523			8. Performing Organization Rept. No. CER81-82KMK-RNM9	
12. Sponsoring Organization Name and Address Gas Research Institute 8600 West Bryn Mawr Avenue Chicago, Illinois 60613			10. Project/Task/Work Unit No. 5014-352-0203	
15. Supplementary Notes			11. Contract(C) or Grant(G) No. (C) (G)	
16. Abstract (Limit: 200 words) A wind-tunnel test program was conducted on a 1:250 scale model to determine the effects of fences and vortex generators on the dispersion of LNG plumes. The tests were conducted simulating continuous LNG boiloff rates of 20, 30 and 40 m ³ /min; 4, 7, 9 and 12 m/sec wind speed for fence data and 4, 7 and 9 m/sec wind speed for vortex generator data; six configurations; and two heights of fences and vortex generators. Plots of ground-level mean concentration contours were constructed. The highest concentrations were observed for the case of no fences and vortex generators. Fences and vortex generators created higher turbulence intensity in the wake and resulted into enhanced mixing thus reducing the ground-level hazards of LNG plumes. In general, the lower wind speed gave the higher ground-level concentration when fence or vortex generator interacted with the LNG plume. However, for the case of no fence or vortex generator the higher concentration persisted for longer downwind distances for 7 m/sec wind speed. As expected, the ground-level concentrations were increased with an increase in LNG boiloff rate but decreased with the increase in the fence/vortex generator height. In general, the solid fences gave the lower ground-level concentration as compared with the vortex generator with identical conditions. The double fences or vortex generators gave the maximum LNG plume dilution. However, the single fence or vortex generator near the source gave approximately the same dilution and hence, it would not justify the additional expenses of having second fence or vortex generator. It was also observed that the maximum LNG plume dilution occurs when the fence or vortex generator is closest possible to the LNG spill area.			13. Type of Report & Period Covered Final (August 1981 - May 1982)	
17. Document Analysis a. Descriptors Liquefied Natural Gas, Wind tunnel, Dispersion of heavy plume, Fences, Vortex generators, Turbulent boundary layer.			14.	
b. Identifiers/Open-Ended Terms				
c. COSATI Field/Group				
18. Availability Statement: Distribution unlimited		19. Security Class (This Report) Unclassified		21. No. of Pages 88
		20. Security Class (This Page) Unclassified		22. Price

RESEARCH SUMMARY

Title Accelerated Dilution of Liquefied Natural Gas Plumes with Fences and Vortex Generators

Contractor Civil Engineering Department
Colorado State University
Fort Collins, Colorado 80523

GRI Contract Number: 5014-352-0203

Principal Investigators K. M. Kothari and R. N. Meroney

Report Period August 1981 - May 1982
Final Report

Objective To determine, through utilization of wind-tunnel experiments, the effects of fences and vortex generators on the dilution of Liquefied Natural Gas plumes.

Technical Perspective A Liquefied Natural Gas (LNG) spill would result in a cold LNG vapor plume, remaining negatively buoyant for a long period of time. The LNG plume could be diluted utilizing passive systems such as a fence or a vortex generator at or near the LNG spill location. There is a need for determining how these devices interact with a LNG plume, the optimal sizes and configurations, and the resultant dilution factors achievable under various wind speeds and LNG boiloff rates.

Results A large data base on the interaction of LNG plumes with fences and vortex generators was obtained. The wind-tunnel experiments included three simulated LNG

boiloff rates, four wind speeds, six configurations of fences or vortex generators as accelerating devices for dilution, and two heights for each device. The effects of the variations of these parameters on LNG plume dispersion were obtained. An empirical description of the continuous plume tests was developed and advantages of accelerating devices are discussed.

Technical Approach

Wind-tunnel tests were performed at a scale of 1:250 to determine the accelerated dispersion of a LNG plume as a result of interaction with fences or vortex generators. An LNG plume is heavier than air at boiloff conditions, and is anticipated to remain negatively buoyant for most conditions until it is adequately dispersed. The negatively buoyant plume condition can be simulated in the wind-tunnel by using an isothermal heavy gas of molecular weight equal to that of LNG at boiloff. The measured results should be modified to account for the difference in moles of cold gas vs. the moles in isothermal gas. The fences and vortex generators of various sizes and shapes were constructed from aluminium plate and heavy gases were introduced into the wind tunnel via an area source of constant diameter mounted flush on the wind-tunnel floor. The wind tunnel floor was level and smooth for all tests. Gas concentration samples were collected

downwind of the area source under various conditions. These samples were analyzed using a gas chromatograph and from this data the plume structure was determined.

Project
Implications

This task of the wind-tunnel test program has shown that a passive fence or vortex generator can have a significant effect on vapor cloud dispersion. They have excellent promise for practical use in ensuring the necessary dilution of LNG vapor clouds in the event of an accidental spill. GRI will use the data obtained to assess the capability of numerical vapor dispersion models in predicting the functional relation between spill size, wind speed, fence characteristics, and downwind dispersion distances. The theoretical model and the wind-tunnel results can then be used to design larger-scale tests to validate wind-tunnel and model results. The end objective is explicit design guidelines for fences or vortex generators for LNG facilities.

GRI Project Manager
Steve J. Wiersma
Environment and Safety Department

<u>Section</u>	TABLE OF CONTENTS	<u>Page</u>
GRI DISCLAIMER		i
RESEARCH SUMMARY		ii
LIST OF TABLES		vi
LIST OF FIGURES		vii
LIST OF SYMBOLS		x
1.0 INTRODUCTION		1
2.0 MODELING OF PLUME DISPERSION		4
2.1 PHYSICAL MODELING OF THE ATMOSPHERIC BOUNDARY LAYER		5
2.1.1 Partial Simulation of the Atmospheric Boundary Layer		6
2.2 PHYSICAL MODELING OF LNG PLUME MOTION		8
2.2.1 Partial Simulation of the Plume Motion		9
2.3 MODELING OF PLUME DISPERSION FOR PRESENT STUDY		15
2.3.1 Physical Modeling of the Atmospheric Surface Layer		15
2.3.2 Physical Modeling of the LNG Spill Plume		16
3.0 DATA AQUISITION AND ANALYSIS		20
3.1 WIND-TUNNEL FACILITIES		20
3.2 MODEL		20
3.3 FLOW VISUALIZATION TECHNIQUES		22
3.4 WIND PROFILE AND TURBULENCE MEASUREMENTS		25
3.5 CONCENTRATION MEASUREMENTS		28
3.5.1 Gas Chromatograph		28
3.5.2 Sampling System		30
3.5.3 Test Procedure		31
4.0 TEST PROGRAM		33
4.1 Results and Discussion		39
4.1.1 Approach Velocities		39
4.1.2 Flow Visualization Results		39
4.1.3 Concentration Measurement Results		44
5.0 CONCLUSIONS		81
REFERENCES		83
APPENDIX A - THE CALCULATION OF MODEL-SCALE FACTORS		86

LIST OF TABLES

<u>Table</u>		<u>Page</u>
1	Summary of Tests (Fence Data)	35
2	Summary of Tests (Vortex Generator Data)	36
3	Summary of Plane Area Source Data	70
4	Summary of Fence Data at the Wind Speed of 4 m/sec	71
5	Summary of Fence Data at the Wind Speed of 7 m/sec	72
6	Summary of Fence Data at the Wind Speed of 9 m/sec	73
7	Summary of Fence Data at the Wind Speed of 12 m/sec	74
8	Summary of Vortex Generator Data at the Wind Speed of 4 m/sec	75
9	Summary of Vortex Generator Data at the Wind Speed of 7 m/sec	76
10	Summary of Vortex Generator Data at the Wind Speed of 9 m/sec	77

LIST OF FIGURES

<u>Figure</u>		<u>Page</u>
1	Specific Gravity of LNG Vapor - Humid Atmospheric Mixtures	13
2	Variation of Isothermal Plume Behavior from Equivalent Cold Methane Plume Behavior	18
3	Environmental Wind Tunnel	21
4	Model Fences	23
5	Model Vortex Generators	24
6	Velocity Probes and Velocity Standard	26
7	Velocity Data Reduction Flowchart	27
8	Photographs of (a) the Gas Sampling System, and (b) the HP Integrator and Chromatograph	29
9	Concentration Measurement Locations and Configuration 0 Identification	34
10	Configurations 1 to 3 Identification	37
11	Configurations 4 to 6 Identification	38
12	Mean Velocity and Turbulence Intensity Profiles for Equivalent Prototype Wind Speed of 4 m/sec at 10 m Height	40
13	Mean Velocity and Turbulence Intensity Profiles for Equivalent Prototype Wind Speed of 7 m/sec at 10 m Height	41
14	Mean Velocity and Turbulence Intensity Profiles for Equivalent Prototype Wind Speed of 9 m/sec at 10 m Height	42
15	Mean Velocity and Turbulence Intensity Profiles for Equivalent Prototype Wind Speed of 12 m/sec at 10 m Height	43
16	Flow visualization (a) No Fence or Vortex Generator; (b) 4 cm (10 m) Height Fence, Configuration 1; (c) 4 cm (10 m) Height Vortex Generator, Configuration 4; Equivalent Wind Speed 7 m/sec at 10 m Height, Equivalent LNG Boiloff rate of 40 m ³ /min	45
17	Ground-level Mean Concentration Isopleths for Run Number 1	46

<u>Figure</u>	<u>Page</u>
18 Ground-level Mean Concentration Isopleths for Run Number 2	47
19 Ground-level Mean Concentration Isopleths for Run Number 3	48
20 Ground-level Mean Concentration Isopleths for Run Number 5	49
21 Ground-level Mean Concentration Isopleths for Run Number 6	50
22 Ground-level Mean Concentration Isopleths for Run Number 10	51
23 Ground-level Mean Concentration Isopleths for Run Number 14	52
24 Ground-level Mean Concentration Isopleths for Run Number 18	53
25 Ground-level Mean Concentration Isopleths for Run Number 19	54
26 Ground-level Mean Concentration Isopleths for Run Number 20	55
27 Ground-level Mean Concentration Isopleths for Run Number 26	56
28 Ground-level Mean Concentration Isopleths for Run Number 40	57
29 Ground-level Mean Concentration Isopleths for Run Number 58	58
30 Ground-level Mean Concentration Isopleths for Run Number 74	59
31 Ground-level Mean Concentration Isopleths for Run Number 91	60
32 Ground-level Mean Concentration Isopleths for Run Number 154	61
33 Ground-level Mean Concentration Isopleths for Run Number 169	62
34 Ground-level Mean Concentration Isopleths for Run Number 172	63

<u>Figure</u>		<u>Page</u>
35	Ground-level Mean Concentration Isopleths for Run Number 173	64
36	Ground-level Mean Concentration Isopleths for Run Number 174	65
37	Ground-level Mean Concentration Isopleths for Run Number 175	66
38	Ground-level Mean Concentration Isopleths for Run Number 181	67
39	Ground-level Mean Concentration Isopleths for Run Number 190	68

LIST OF SYMBOLS

Dimensions are given in terms of mass (m), length (L), time (t), moles (n), and temperature (T).

<u>Symbol</u>	<u>Definition</u>	
A	Area	$[L^2]$
C_p	Specific heat capacity at constant pressure	$[L^2 t^{-2} T^{-1}]$
C_p^*	Molar specific heat capacity at constant pressure	$[L^2 m t^{-2} T^{-1} n^{-1}]$
D	Source diameter	$[L]$
g	Gravitational acceleration	$[L t^{-2}]$
h	Local plume depth	$[L]$
k	Thermal conductivity	$[m L T^{-1} t^{-3}]$
L	Length	$[L]$
M	Molecular weight	$[m n^{-1}]$
Ma	Mach number	
n	Mole	$[n]$
p	Velocity power law exponent	
Q	Volumetric rate of gas flow	$[L^3 t^{-1}]$
T	Temperature	$[T]$
ΔT	Temperature difference across some reference layer	$[T]$
t	Time	$[t]$
u_x	Friction velocity	$[L t^{-1}]$
U	Velocity	$[L t^{-1}]$
V	Volume	$[L^3]$
W	Plume vertical velocity	$[L t^{-1}]$
x	General downwind coordinate	$[L]$
y	General lateral coordinate	$[L]$
z	General vertical coordinate	$[L]$

LIST OF SYMBOLS (continued)

<u>Symbol</u>	<u>Definition</u>	
z_o	Surface roughness parameter	[L]
δ	Boundary layer thickness	[L]
Λ	Integral length scale of turbulence	[L]
$\Delta\rho$	Density difference between source gas and air	[mL ⁻³]
ρ	Density	[mL ⁻³]
σ	Standard deviation	
χ	Mole fraction of gas component	
Ω	Angular velocity of earth = 0.726×10^{-4} (radians/sec)	[t ⁻¹]
λ_p	Peak wavelength	[L]
	Kinematic viscosity	[L ² t ⁻¹]

Subscripts and Abbreviations

b.o.	Boiloff
g	Gas
i	Cartesian index
LNG	Liquefied Natural Gas
m	Model
NG	Natural gas
o	Reference conditions
p	Prototype
s	Source gas

1.0 INTRODUCTION

Natural gas is a highly desirable form of energy for consumption in the United States. A sophisticated distribution network already services a major part of the country. Recent efforts to expand this nation's natural gas supply include the transport of natural gas in a liquid state from distant gas fields. Also, about 100 peak shaving plants exist where gas is liquefied during slack periods and vaporized for distribution during peak use periods. Liquefied Natural Gas (LNG) is transported and stored at about -162°C . At this temperature if a storage tank on a ship or land were to rupture and the contents spill out, rapid boiling of the LNG would ensue and the liberation of a potentially flammable vapor would result. It is envisioned that if the flow from a rupture in a typical full LNG storage tank could not be constrained, up to 28 million cubic meters of LNG would be released in 80 minutes [1]. Past studies [1,2] have demonstrated that, for most atmospheric conditions the cold LNG vapor plume will remain negatively buoyant until it is adequately dispersed; thus, it represents a ground-level hazard. This hazard will extend downwind until the atmosphere has diluted the LNG vapor below the lower flammability limit (a local concentration for methane below 5 percent by volume).

It is important that accurate predictive models for LNG vapor cloud physics be developed, so that the associated hazards of transportation and storage may be evaluated. Various industrial and governmental agencies have sponsored analytical, empirical, and physical modeling studies to analyze problems associated with the transportation and storage of LNG as well as other liquefied gaseous fuels. Since these models require assumptions to permit tractable solution, one must perform atmospheric scale tests to verify the accuracy of these models.

A multitask research program has been designed by a combined Gas Research Institute (GRI)/Department of Energy (DOE) effort to address the problem of predictive methods in LNG hazard analysis. One aspect of this program is the physical simulation of LNG vapor dispersion in a meteorological wind tunnel. The complete sub-program research contract, GRI contract number 5014-352-0203 consists of five tasks.

Task 1: Laboratory Support Tests for the Forty Cubic Meter LNG Spill Series at China Lake, California.

Task 2: Physical Simulation in Laboratory Wind Tunnels of the 1981 LNG Spill Tests performed at China Lake, California.

Task 3: Laboratory Simulation of Idealized Spills on Land and Water.

Task 4: Laboratory Tests Defining LNG Plume Interaction with Surface Obstacles.

Task 5: Laboratory Tests to Determine the Accelerated Dilution of a LNG Plume by Fences and Vortex Generators near the LNG Source.

Tasks 1 and 2 were presented in the July 1980 and July 1981 annual reports, respectively. Task 2 is also the subject of a final report to GRI by Neff et al. (1981) [3]. Task 3 report has been presented by Neff et al. [4]. Task 4, the LNG plume interaction with surface obstacles has been reported by Kothari et al. [5]. Task 5, the accelerated dilution of LNG plume due to fences and vortex generators is the sole subject of this report.

Some experts currently assume that considerable mixing takes place during gravity driven vapor spreading; whereas others assume no dilution of vapors during this stage of dispersion. It is not surprising then

that models based on such a wide variation of assumptions concerning the kinematics of plume development predict distances to Lower Flammability Limit (LFL) ranging from fractions to tens of miles for the same spill conditions.

None of the current dispersion models incorporate the additional complications of buildings, fences and vortex generators. Such interference may cause additional plume dilution or temporary pooling of high gas concentrations. The purpose of this study was to develop, through the use of atmospheric boundary layer wind tunnels, empirical appreciation of the physics of LNG plume interaction with fences and vortex generators. For fences, four wind speeds, three fence configurations, three LNG boiloff rates, and two fence heights were examined in the wind tunnel. For vortex generators, three wind speeds, three vortex generator configurations, three LNG boiloff rates, and two vortex generator heights were examined. Additional tests were conducted without a fence or a vortex generator for three boiloff rates and four wind speeds for comparison with the fence or vortex generator data. The total of 138 tests were performed during the course of the research.

The wind-tunnel test program was conducted on a 1:250 scale model of various configurations. The program consisted of continuous releases of a LNG plume and the subsequent measurement of ground-level concentrations up to 500 m scaled downwind distance.

The methods employed in the physical modeling of atmospheric and plume motion are discussed in Chapter 2. The details of model construction and experimental measurements are described in Chapter 3. Chapter 4 discusses the test program and results. Chapter 5 summarizes the conclusions of this research.

2.0 MODELING OF PLUME DISPERSION

To obtain a predictive model for a specific plume dispersion problem one must quantify the pertinent physical variables and parameters into a logical expression that determines their interrelationships. This task is achieved implicitly for processes occurring in the atmospheric boundary layer by the formulation of the equations of conservation of mass, momentum, and energy. These equations with site and source conditions and associated constitutive relations are highly descriptive of the actual physical interrelationship of the various independent (spill size or spill rate, space and time) and dependent (velocity, temperature, pressure, density, etc.) variables.

These generalized conservation statements subjected to the typical boundary conditions of atmospheric flow are too complex to be solved by present analytical or numerical techniques. It is also unlikely that one could create a physical model for which exact similarity exists for all the dependent variables over all the scales of motion present in the atmosphere. Thus, one must resort to various degrees of approximation to obtain a predictive model. At present, purely analytical or numerical solutions of plume dispersion are unavailable because of the classical problem of turbulent closure [6]. Such techniques rely heavily upon empirical input from observed or physically modeled data. The combined empirical-analytical-numerical solutions have been combined into several different predictive approaches by Pasquill [7] and others. The estimates of dispersion by these approaches are often crude; hence, they should only be used when the approach and site terrain are uniform and without obstacles such as fences, buildings or vortex generators. Boundary layer wind tunnels are capable of physically modeling plume

processes in the atmosphere under certain restrictions. These restrictions are discussed in the next few sections.

2.1 PHYSICAL MODELING OF THE ATMOSPHERIC BOUNDARY LAYER

The atmospheric boundary layer is that portion of the atmosphere extending from ground level to a height of approximately 100 meters within which the major exchanges of mass, momentum, and heat occur. This region of the atmosphere is described mathematically by statements of conservation of mass, momentum, and energy [8]. The general requirements for laboratory-atmospheric-flow similarity may be obtained by fractional analysis of these governing equations [9]. This methodology is accomplished by scaling the pertinent dependent and independent variables and then casting the equations into dimensionless form by dividing by one of the coefficients (the inertial terms in this case). Performing these operations on such dimensional equations yields dimensionless parameters commonly known as:

Reynolds number	$Re = U_0 L_0 / \nu_0$	$= \frac{\text{Inertial Force}}{\text{Viscous Force}}$
Bulk Richardson number	$Ri = [(\Delta T)_0 / T_0] (L_0 / U_0^2) g_0$	$= \frac{\text{Gravitational Force}}{\text{Inertial Force}}$
Rossby number	$Ro = U_0 / L_0 \Omega_0$	$= \frac{\text{Inertial Force}}{\text{Coriolis Force}}$
Prandtl number	$Pr = \nu_0 / (k_0 / \rho_0 c_{p_0})$	$= \frac{\text{Viscous Diffusivity}}{\text{Thermal Diffusivity}}$
Eckert number	$Ec = U_0^2 / c_{p_0} (\Delta \bar{T})_0$	

For exact similarity between different flows which are described by the same set of equations, each of these dimensionless parameters must be equal for both flow systems. In addition to this requirement, there must be similarity between the surface-boundary conditions.

Surface-boundary condition similarity requires equivalence of the following features:

- a. Surface-roughness distributions,
- b. topographic relief, and
- c. surface-temperature distribution.

If all the foregoing requirements are met simultaneously, all atmospheric scales of motion ranging from micro to mesoscale could be simulated within the same flow field for a given set of boundary conditions [10]. However, all of the requirements cannot be satisfied simultaneously by existing laboratory facilities; thus, a partial or approximate simulation must be used. This limitation requires that atmospheric simulation for a particular application must be designed to simulate most accurately those scales of motion which are of greatest significance for the given application.

2.1.1 Partial Simulation of the Atmospheric Boundary Layer

A partial simulation is practically realizable only because the kinematics and dynamics of flow systems above a certain minimum Reynolds number are independent of its magnitude [11,12]. The magnitude of the minimum Reynolds number will depend upon the geometry of the flow system being studied. Halitsky [13] reported that for concentration measurements on a cube placed in a near uniform flow field the Reynolds number required for invariance of the concentration distribution over the cube surface and downwind must exceed 11,000. Because of this invariance, exact similarity of Reynolds parameter is neglected when physically modeling the atmosphere.

When the flow scale being modeled is small enough such that the turning of the mean wind directions with height is unimportant,

similarity of the Rossby number may be relaxed. For the case of dispersion of LNG plume near the ground level the Coriolis effect on the plume motion would be extremely small.

The Eckert number for air is equivalent to $0.4 \text{ Ma}^2 \left(\frac{T_0}{\Delta T_0} \right)$ where Ma is the Mach number [6]. For the wind velocities and temperature differences which occur in either the atmosphere or the laboratory flow the Eckert number is very small; thus, the effects of energy dissipation with respect to the convection of energy is negligible for both model and prototype. Eckert number equality is relaxed.

Prandtl number equality is easily obtained since it is dependent on the molecular properties of the working fluid which is air for both model and prototype.

Bulk Richardson number equality may be obtained in special laboratory facilities such as the Meteorological Wind Tunnel at Colorado State University [14].

Quite often during the modeling of a specific flow phenomenon it is sufficient to model only a portion of a boundary layer or a portion of the spectral energy distribution. This relaxation allows more flexibility in the choice of the length scale that is to be used in a model study. When this technique is employed it is common to scale the flow by any combination of the following length scales, δ , the portion of the boundary layer to be simulated; z_0 , the aerodynamic roughness; Λ_i , the integral length scale of the velocity fluctuations, or λ_p , the wavelength at which the peak spectral energy is observed.

Unfortunately many of the scaling parameters and characteristic profiles are difficult to obtain in the atmosphere. They are infrequently known for many of the sites to which a model study is to

be performed. To help alleviate this problem Counihan [15] has summarized measured values of some of these different parametric descriptions for the atmospheric flow at many different sites and flow conditions.

2.2 PHYSICAL MODELING OF LNG PLUME MOTION

In addition to modeling the turbulent structure of the atmosphere in the vicinity of a test site it is necessary to scale the LNG plume source conditions properly. One approach would be to follow the methodology used in Section 2.1, i.e., writing the conservation statements for the combined flow system followed by fractional analysis to find the governing parameters. An alternative approach, the one which will be used here, is that of similitude [9]. The method of similitude obtains scaling parameters by reasoning that the mass ratios, force ratios, energy ratios, and property ratios should be equal for both model and prototype. When one considers the dynamics of gaseous LNG plume behavior the following nondimensional parameters of importance are identified [13,14,16,17,18].^{1,2}

$$\text{Mass Ratio} = \frac{\text{mass flow of LNG plume}}{\text{effective mass flow of air}}$$

$$= \frac{\rho_s W_s A_s}{\rho_a U_a A_a} = \frac{\rho_s Q}{\rho_a U_a L^2}$$

¹It has been assumed that the dominant transfer mechanism is that of turbulent entrainment. Thus the transfer processes of heat conduction, convection, and radiation are negligible.

²The scaling of plume Reynolds number is also a significant parameter. Its effects are invariant over a large range thus making it possible to scale the distribution of mean and turbulent velocities and relax exact parameter equality.

$$\begin{aligned}
 \text{Momentum Ratio} &= \frac{\text{inertia of LNG plume}}{\text{effective inertia of air}} \\
 &= \frac{\rho_s W_s^2 A_s}{\rho_a U_a^2 A_a} = \frac{\rho_s Q^2}{\rho_a U_a^2 L^4} \\
 \text{Densimetric Froude No. (Fr)} &= \frac{\text{effective inertia of air}}{\text{buoyancy of LNG plume}} \\
 &= \frac{\rho_a U_a^2 A_a}{g(\rho_g - \rho_a)V_s} = \frac{U_a^2}{g\left(\frac{\rho_s - \rho_a}{\rho_a}\right)L} \\
 \text{Volume Flux Ratio} &= \frac{\text{volume flow of LNG plume}}{\text{effective volume flow of air}} \\
 &= \frac{Q}{UL^2}
 \end{aligned}$$

To obtain simultaneous simulation of these four parameters at a reduced geometric scale it is necessary to maintain equality of the LNG plume specific gravity ρ_s/ρ_a .

2.2.1 Partial Simulation of LNG Plume Motion

The restriction to an exact variation of the density ratio for the entire life of a plume is difficult to meet for LNG plumes which simultaneously vary in molecular weight and temperature. To emphasize this point more clearly, consider the mixing of two volumes of gas, one being the source gas, V_s , the other being ambient air, V_a . Consideration of the conservation of mass and energy for this system yields [19]¹:

$$\frac{\rho_g}{\rho_a} = \frac{\frac{\rho_s}{\rho_a} V_s + V_s}{\left(\frac{T_a}{T_s} V_s + V_a\right) \left(\frac{C_{p_s} M_s}{C_{p_a} M_a} V_s + V_a\right) \left(\frac{C_{p_s} M_s T_a}{C_{p_a} M_a T_s} V_s + V_a\right)}$$

¹The pertinent assumption in this derivation is that the gases are ideal and properties are constant.

If the temperature of the air, T_a , equals the temperature of the source gases, T_s , or if the product, $C_p M$, is equal for both source gas and air then the equation reduces to:

$$\frac{\rho_g}{\rho_a} = \frac{\frac{\rho_s}{\rho_a} V_s + V_a}{V_s + V_a} \quad (2-8)$$

Thus for two prototype cases: 1) an isothermal plume and 2) a thermal plume which is mostly composed of air, it does not matter how one models the density ratio as long as the initial density ratio value is equal for both model and prototype.

For a plume whose temperature, molecular weight, and specific heat are all different from that of the ambient air, i.e., a cold natural gas plume, equality in the variation of the density ratio upon mixing must be relaxed slightly if one is to model utilizing a gas different from that of the prototype.¹ In most situations this deviation from exact similarity is small (see discussion Section 2.3.2).

Scaling of the effects of heat transfer by conduction, convection, or radiation cannot be reproduced when the model source gas and environment are isothermal. Fortunately in a large majority of industrial plumes the effects of heat transfer by conduction, convection, and radiation from the environment are small enough that the plume buoyancy remains essentially unchanged. In the specific case of a cryogenic liquid spill the influence of heat transfer on cold dense gas dispersion can be divided into two phases. First, the temperature (and hence specific gravity) of the plume at exit from a containment tank and

¹If one were to use a gas whose temperature is different from that of the ambient air then consideration of similarity in the scaling of the energy ratios must be considered.

surrounding dike area is dependent on the thermal diffusivity of the tank-dike-spill surface materials, the volume of the tank-dike structure, the actual boiloff rate, and details of the spill surface geometry. A second plume phase involves the heat transfer from the ground surface beyond the spill area into the plume which lowers plume density.

It would be desirable to simulate the entire transient spill phenomenon in the laboratory including spill of cryogenic fluid into the dike, heat transfer from the tank and dike materials to the cryogenic fluid, phase change of the liquid and subsequent downwind dispersal of cold gas. Unfortunately, the different scaling laws for the conduction and convection require markedly different time scales for the various processes as the length scale changes. Since the volume of dike material storing sensible heat scales as the cube of length whereas the pertinent surface area scales as the square of length heat is transferred to a model cold plume much too rapidly within the model containment structures. This effect is apparently unavoidable since a material having a thermal diffusivity low enough to compensate for this effect does not appear to exist. Calculations for the full-scale situation suggest minimal heating of a cold gas plume by the tank-dike structure thus it may suffice to cool the model tank-dike walls to reduce the heat transfer to a cold model vapor and study the resultant cold plume.

Boyle and Kneebone [19] released room temperature propane and LNG onto a water surface under equivalent conditions. The density of propane at ambient temperatures and methane at -161°C are the same. Using the modified Froude number as a model law they concluded dispersion characteristics were equivalent within experimental error.

A mixture of 50% helium and 50% nitrogen pre-cooled to 115°K was released from model tank-dike systems by Meroney et al. [20], to simulate equivalent LNG spill behavior. It was expected the gross influences of different heat transfer conditions could be determined, however, there was no guarantee that these experiments reproduced quantitatively similar situations in the field. Since the turbulence characteristics of the flow are dominated by roughness, upstream wind profile shape, and stratification one expects the Stanton number in the field will equal that in the model, and heat transfer rates in the two cases should be in proper relation to plume entrainment rates. On the other hand, if temperature differences are such that free convection heat transfer conditions dominate, scaling inequalities may exist; nonetheless, model dispersion rates would be conservative.

Visualization experiments performed with equivalent dense isothermal and dense cold plumes revealed no apparent change in plume geometry. Concentration data followed similar trends in both situations. No significant differentiation appeared between insulated versus heat conducting ground surfaces or neutral versus stratified approach flows.

The influence of latent heat release by moisture upon the buoyancy of a plume is a function of the quantity of water vapor present in the plume and the humidity of the ambient atmosphere. Such phase change effects on plume buoyancy can be very pronounced in some prototype situations. Figure 1 displays the variation of specific gravity from a spill of liquefied natural gas in atmospheres of different humidities. For a LNG vapor plume, humidity effects are thus shown to reduce the extent in space and time of plume buoyancy dominance on plume motion. Hence a dry adiabatic model condition should be conservative.

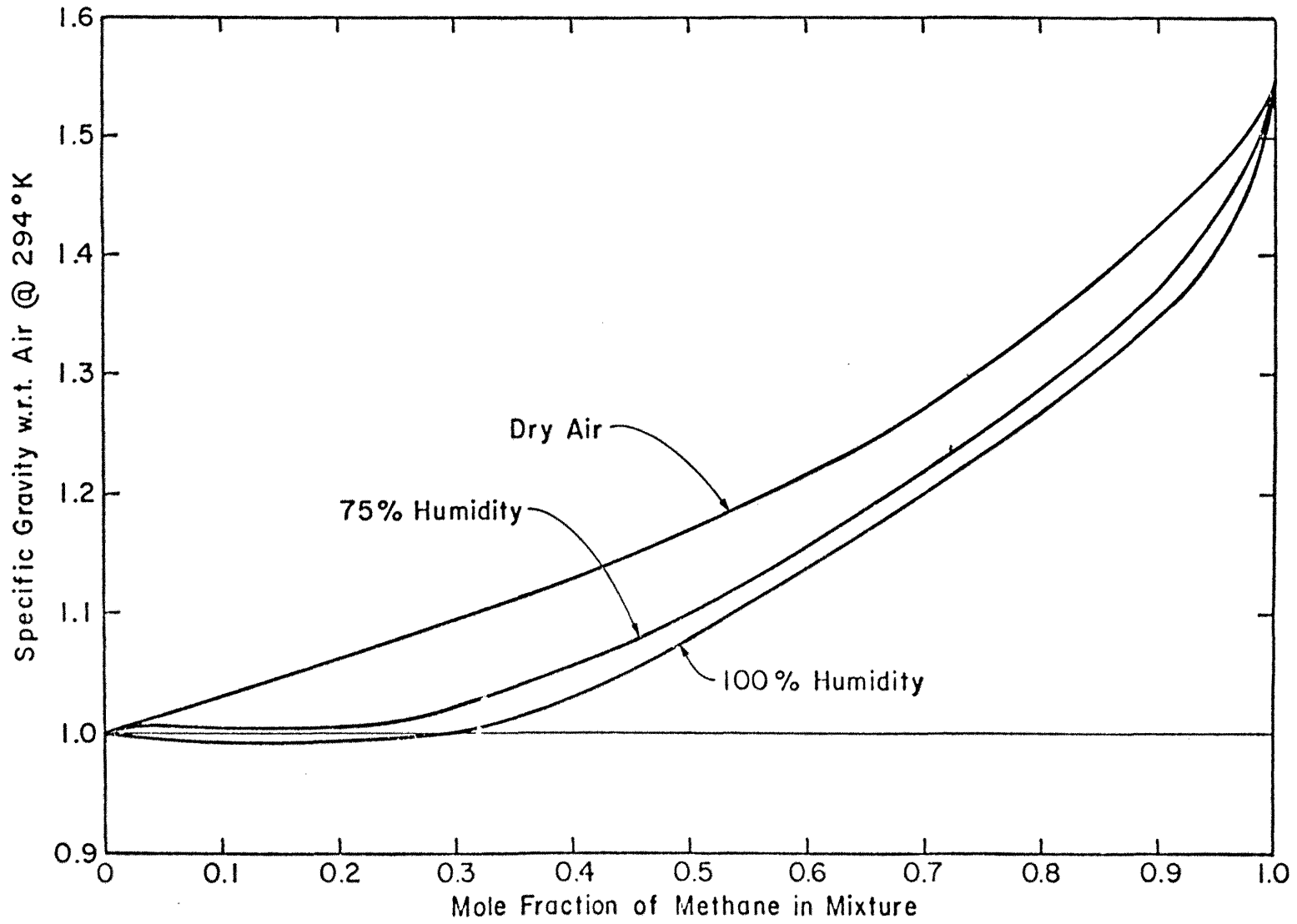


Figure 1. Specific Gravity of LNG Vapor - Humid Atmospheric Mixtures

A reasonably complete simulation may be obtained in some situations even when a modified density ratio ρ_s/ρ_a is stipulated. The advantage of such a procedure is demonstrated most clearly by the statement of equality of Froude Numbers.

$$\left(\frac{U_a^2}{\left(\frac{\rho_s}{\rho_a} - 1\right)Lg} \right)_m = \left(\frac{U_a^2}{\left(\frac{\rho_s}{\rho_a} - 1\right)Lg} \right)_p$$

Solving this equation to find the relationship between model velocity and prototype velocity yields:

$$(U_a)_m = \left(\frac{S.G._m - 1}{S.G._p - 1} \right)^{\frac{1}{2}} \left(\frac{L.S.}{L.S.} \right)^{\frac{1}{2}} (U_a)_p$$

where S.G. is the specific gravity, (ρ_s/ρ_a) , and L.S. is the length scale, (L_p/L_m) . By increasing the specific gravity of the model gas compared to that of the prototype gas, for a given length scale, one increases the reference velocity used in the model. It is difficult to generate a flow which is similar to that of the atmospheric boundary layer in a wind tunnel run at very low wind speeds. Thus the effect of modifying the model specific gravity extends the range of flow situations which can be modeled accurately. But unfortunately during such adjustment of the model gases specific gravity at least two of the four similarity parameters listed must be neglected. The option as to which two of these parameters to retain, if any, depends upon the physical situation being modeled. Two of the three possible options are listed below.

- (1) Froude No. Equality
- Momentum Ratio Equality
- Mass Ratio Inequality
- Velocity Ratio Inequality¹

- (2) Froude No. Equality
- Momentum Ratio Inequality
- Mass Ratio Inequality
- Velocity Ratio Equality

Both of these schemes have been used to model plume dispersion downwind of an electric power plant complex by Skinner [17], Kothari et al. [21], and Meroney [22] respectively.

The modeling of the plume Reynolds number is relaxed in all physical model studies. This parameter is thought to be of small importance since the plume character will be dominated by background atmospheric turbulence soon after its emission. But, if one was interested in plume behavior near the source, then steps should be taken to assure that the model plume is fully turbulent.

2.3 MODELING OF PLUME DISPERSION FOR PRESENT STUDY

In the sections above a review of the extent to which wind tunnels can model LNG plume dispersion in the atmospheric boundary layer has been presented. In this section these arguments will be applied to the case of an LNG spill for the present study.

2.3.1 Physical Modeling of the Atmospheric Surface Layer

The neutral boundary layer was generated in the Environmental Wind Tunnel using spires and a trip at the entrance of the tunnel. The wind speeds were referenced to a 10 m (prototype) height. The aerodynamic roughness, z_0 , and power law exponent, α , were specified such that the boundary layer profile was similar to that expected for a flat suburban terrain area.

¹When this technique is employed, distortion in velocity scales or similarly volume flow rates requires that a correction be applied to the measured concentration field.

2.3.2 Physical Modeling of the LNG Spill Plume

The buoyancy of a plume resulting from an LNG spill is a function of both the mole fraction of methane and temperature. If the plume entrains air adiabatically, then the plume would remain negatively buoyant for its entire lifetime. If the humidity of the atmosphere were high then the buoyancy of the plume will vary from negative to weakly positive. These conclusions are born out in Figure 1, which illustrates the specific gravity of a mixture of methane at boiloff temperature with ambient air and water vapor.

Since the adiabatic plume assumption will yield the most conservative downwind dispersion estimates this situation was simulated. Several investigators have confirmed that the Froude number is the parameter which governs plume spread rate, trajectory, plume size, and entrainment during initial dense plume dilution [5,16,19,23,24]. The modeling of momentum is not of critical importance for a ground source released over a fairly large area. The equality of model and prototype specific gravity was relaxed so that a mixture of ethane and carbon dioxide (specific gravity at 1.5) could be used for the model source gas. The Froude number was maintained at equal values by adjusting reference wind speed.

The use of an isothermal dense model gas such as mixture of ethane and carbon dioxide in place of a cold methane vapor also results in a slight distortion of the local dynamic forces acting on equivalent plume volumes as the gas mixes. Unfortunately this distortion is not conservative, i.e., the thermal capacitance properties of methane result in plumes which behave more dense than the model equivalent plume. Analytical approximations based on the integral entrainment box model of Fay

[25] suggest that buoyancy forces are greater at equivalent time and space positions during adiabatic mixing of methane. Let $Fr = \frac{U(h)^2}{g \frac{\Delta\rho}{\rho_a} h}$ be a local Froude number, where h is local plume depth, $U(h)$ is wind speed at plume depth, h , and $\Delta\rho/\rho_a$ is a local density difference ratio. Then given a power law wind profile $U(h) \sim h^\alpha$ one finds

$$\frac{Fr_{\text{isothermal gas}}}{Fr_{\text{LNG vapor}}} = \frac{(1+\chi S)(\beta+(1-\beta)\theta)}{(\beta(1+\chi S)+(1+S)(1-\beta)\theta)} \left[\frac{(1+\chi S+\chi(1+S)\theta)}{(1-\chi\theta)(1+\chi S)} \right]^{2\alpha} \left[\frac{R_{\text{LNG}}}{R_{\text{iso}}} \right]^{2-4\alpha}$$

where χ = mole fraction methane vapor

R = local plume spread

$\beta = 1 - M_a/M_s \cong -0.81$

$\theta = 1 - T_s/T_a \cong 0.6$

$S = (Cp_s^*/Cp_a^* - 1) \cong 0.22$

α = velocity power law exponent $\cong 0.2$.

The variation of this Froude number ratio with equivalent mole fraction methane is plotted in Figure 2. Nonetheless over most of the concentration range where buoyancy forces are dominant the variation of Froude number is adequately simulated by the isothermal model gas. Indeed, integral-model calculations when corrected for equal mole source strengths predict equal or slightly higher concentration values at equivalent times.

The actual source condition, i.e., the boiloff rate per unit area over the time duration of a spill of LNG on land is highly unpredictable. The source conditions were approximated by assuming a steady boiloff rate of 20, 30 and 40 m³/min over a constant area.

Since the thermally variable prototype gas was simulated by an isothermal simulation gas, the concentration measurements observed in

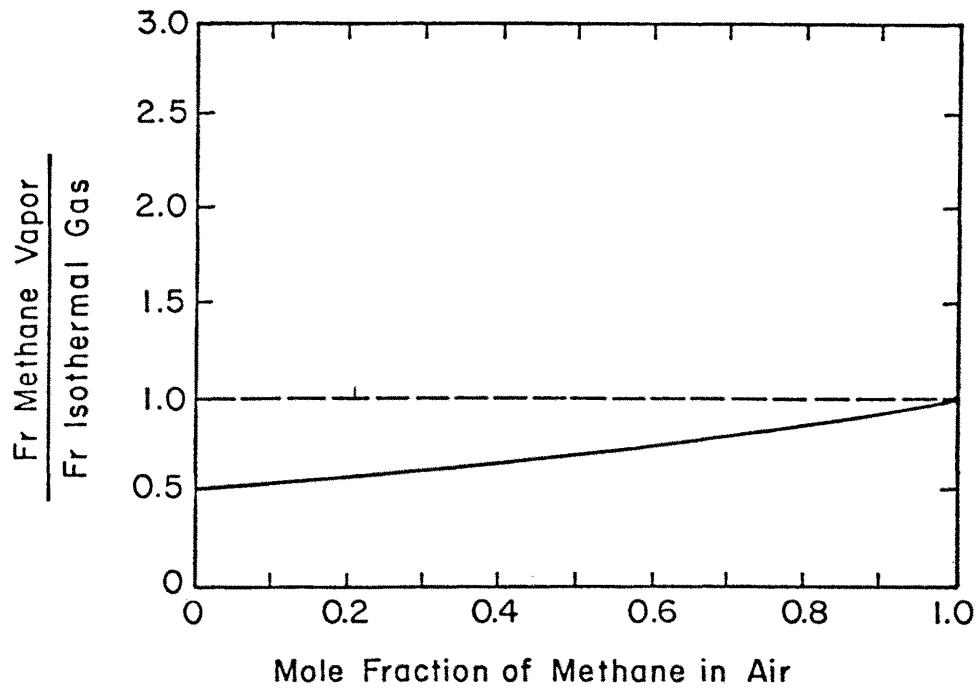


Figure 2. Variation of Isothermal Plume Behavior from Equivalent Cold Methane Plume Behavior

the model must be adjusted to equivalent concentrations that would be measured in the field. This relationship, which is derived in Appendix A, is:

$$x_p = \frac{x_m}{x_m + (1 - x_m) \frac{T_s}{T_a}}$$

where

x_m = volume or mole fraction measured during the model tests,

T_s = source temperature of LNG during field conditions,

T_a = ambient air temperature during field conditions, and

x_p = volume or mole fraction in the field.

3.0 DATA AQUISITION AND ANALYSIS

The methods used to make laboratory measurements and the techniques used to convert these measured quantities to meaningful field-equivalent quantities are discussed in this section. Attention has been drawn to the limitations in the techniques in an attempt to prevent misinterpretation or misunderstanding of the results presented in the next section. Some of the methods used are conventional and need little elaboration.

3.1 WIND-TUNNEL FACILITIES

The Environmental Wind Tunnel (EWT) shown in Figure 3 was used for all tests performed. This wind tunnel, specially designed to study atmospheric flow phenomena, incorporates special features such as adjustable ceiling, rotating turntables, transparent boundary walls, and a long test section to permit reproduction of micrometeorological behavior at larger scales. Mean wind speeds of 0.10 to 12 m/s can be obtained in the EWT. A boundary layer depth of 1 m thickness at 6 m downstream of the test entrance can be obtained with the use of the vortex generators and trip at the test section entrance and surface roughness on the floor. The flexible test section roof on the EWT is adjustable in height to permit the longitudinal pressure gradient to be set to zero. The vortex generators and trip at the tunnel entrance were followed by 8.8 m of smooth floor for the 1:250 scaled area source model.

3.2 MODEL

Based on the previous atmospheric data obtained at sites similar to that of interest in this study it was decided that the best reproduction of the surface wind characteristics would be at a model scale of 1:250. The area source of a scaled diameter of 75 m was constructed from

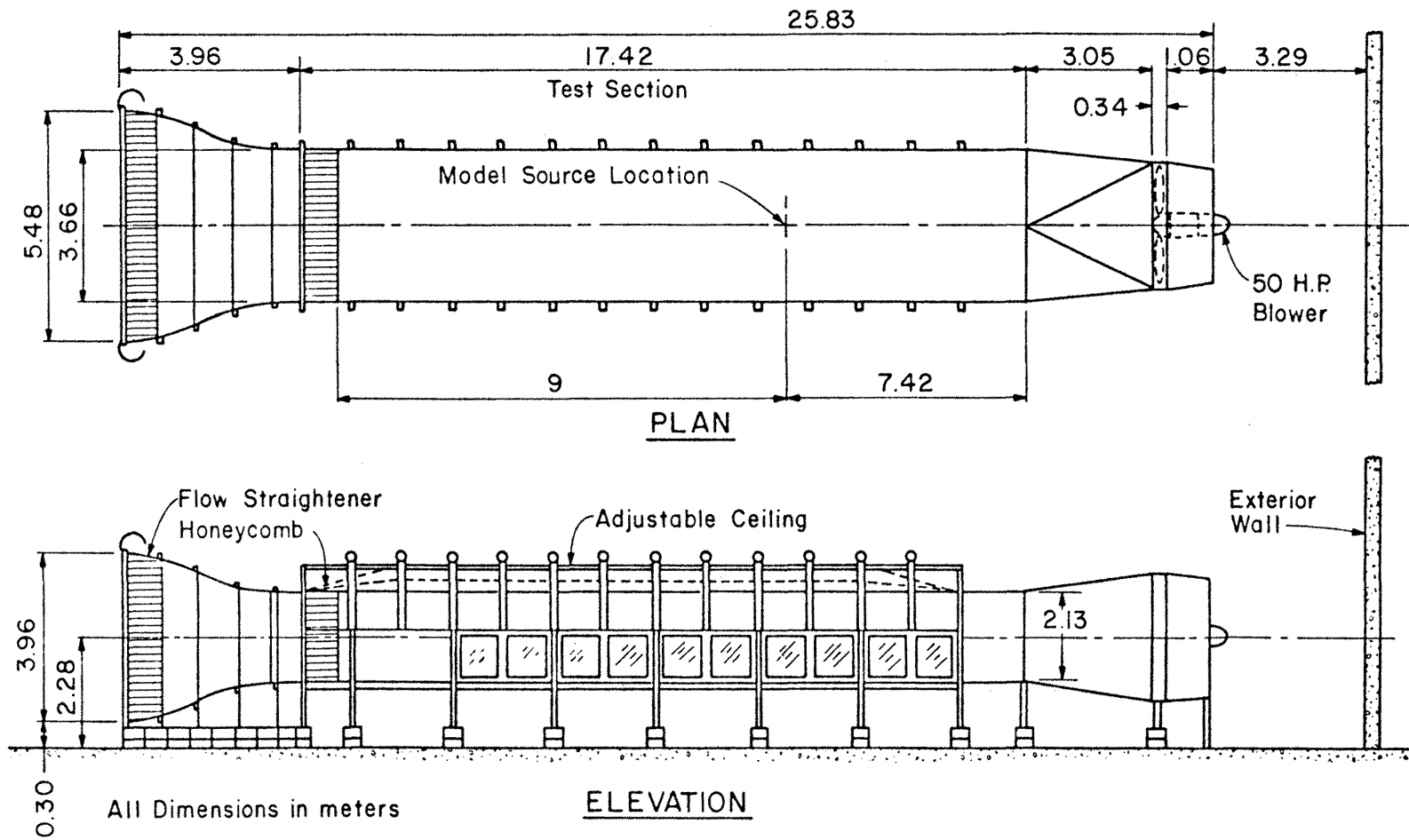


Figure 3. Environmental Wind Tunnel

Plexiglas. The fences and vortex generators were constructed from Aluminium plate of thickness 0.16 cm (1/16 in.). The fences had prototype equivalent dimensions of 75x75x5 m, 150x150x5 m, 75x75x10 m, 150x150x10 m; and vortex generators had prototype equivalent dimensions of 75x75x5 m, 150x150x5 m, 75x75x10 m and 150x150x10 m. The model fences and vortex generators are displayed in Figures 4 and 5, respectively. The model vortex generators were equilateral triangles with,

1. base 7.6 cm, 8 cm height, and tilted to the wind flow at 30° such that the tip of the vortex generator was 4 cm above ground; the spacing between the vortex generator was 2.3 cm,
2. base 3.8 cm, 4 cm height, and tilted to the wind flow at 30° such that the tip of the vortex generator was 2 cm above ground; the spacing between the vortex generator was 2.1 cm.

The source gas, the mixture of 3 percent ethane and 97 percent carbon dioxide, was stored in a high pressured cylinder from which it flowed through a flowmeter and into the circular area source mounted in the wind-tunnel floor.

3.3 FLOW VISUALIZATION TECHNIQUES

Smoke was used to define plume behavior. The smoke was produced by passing the simulation gas through a container of titanium tetrachloride. The plume was illuminated with arc-lamp beams. A visible record was obtained from pictures taken with a Speed Graphic camera utilizing Polaroid film for immediate examination. Additional color slides were obtained with a 35 mm camera; and 16 mm silent movie film was taken with a Bolex motion picture camera.

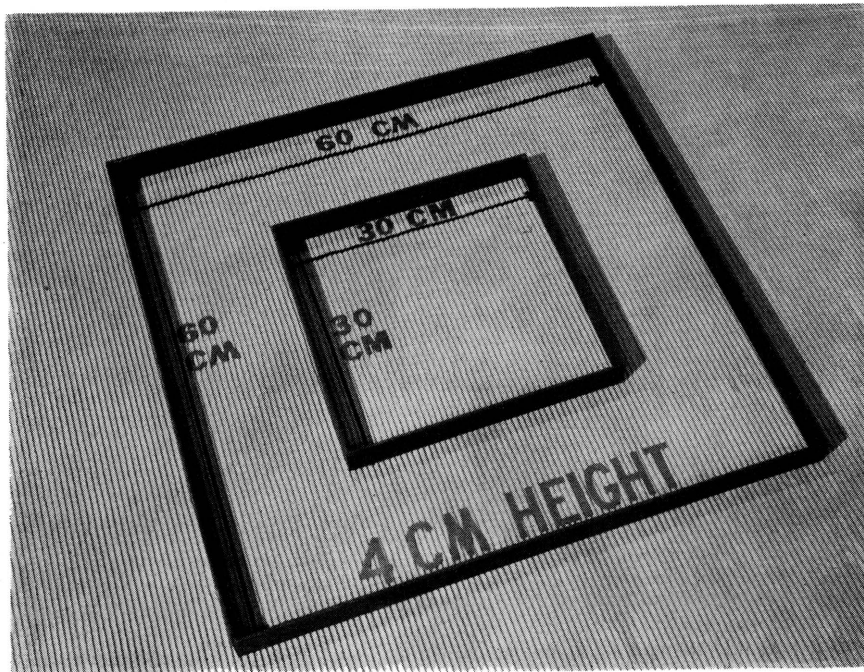
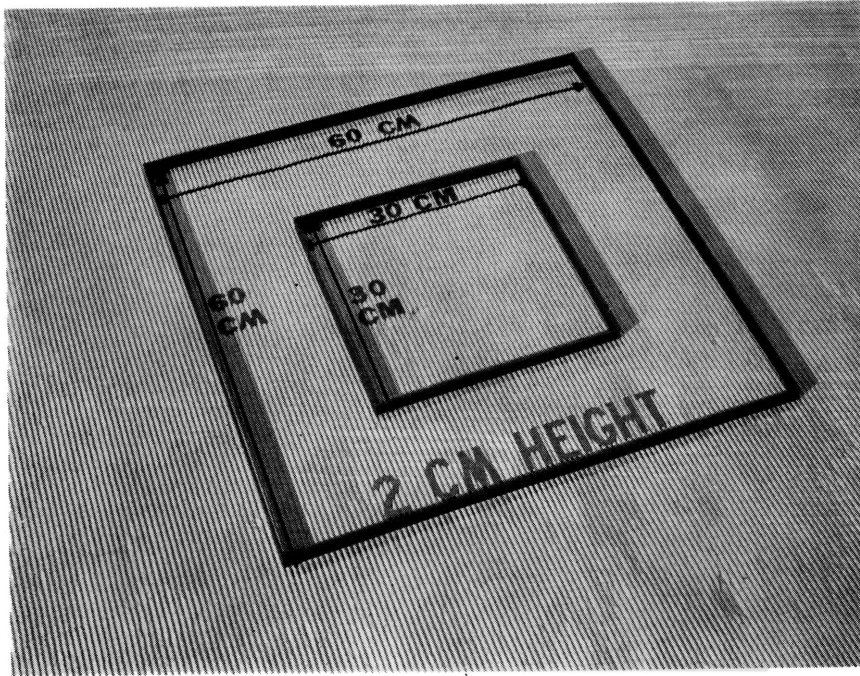


Figure 4. Model Fences

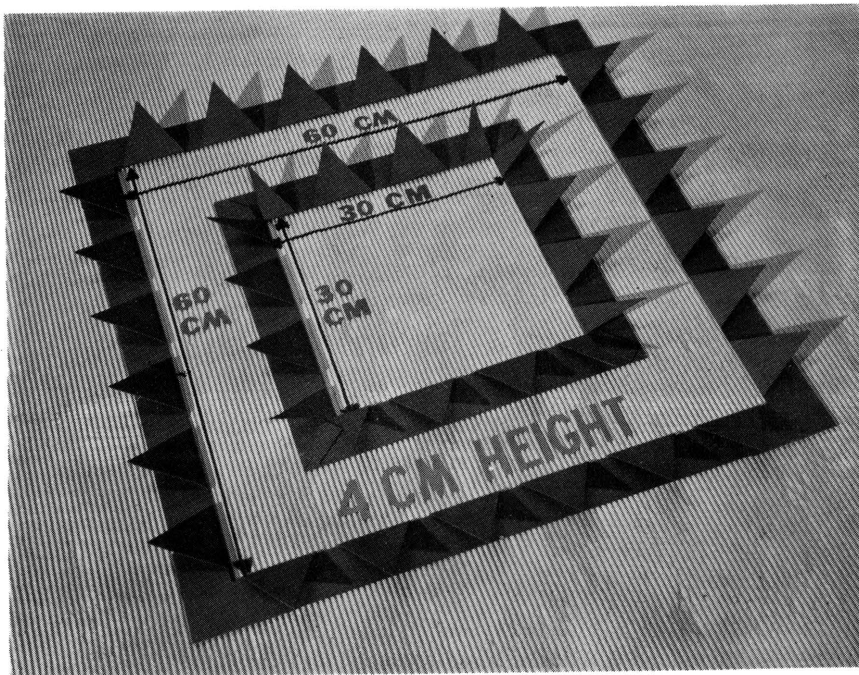
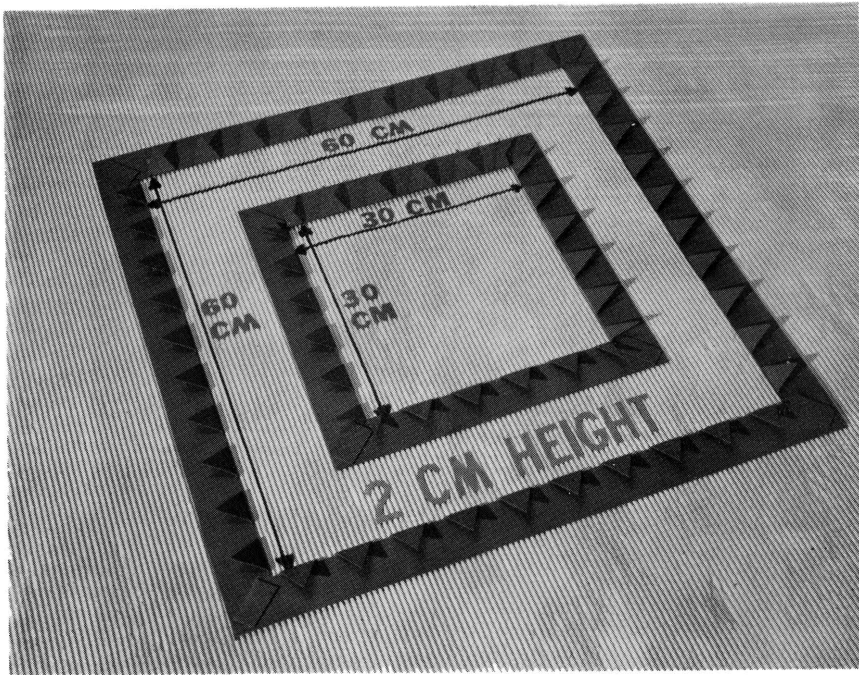


Figure 5. Model Vortex Generators

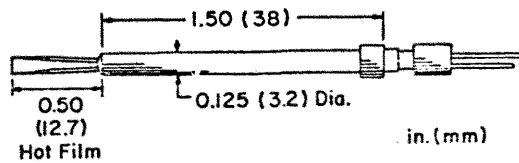
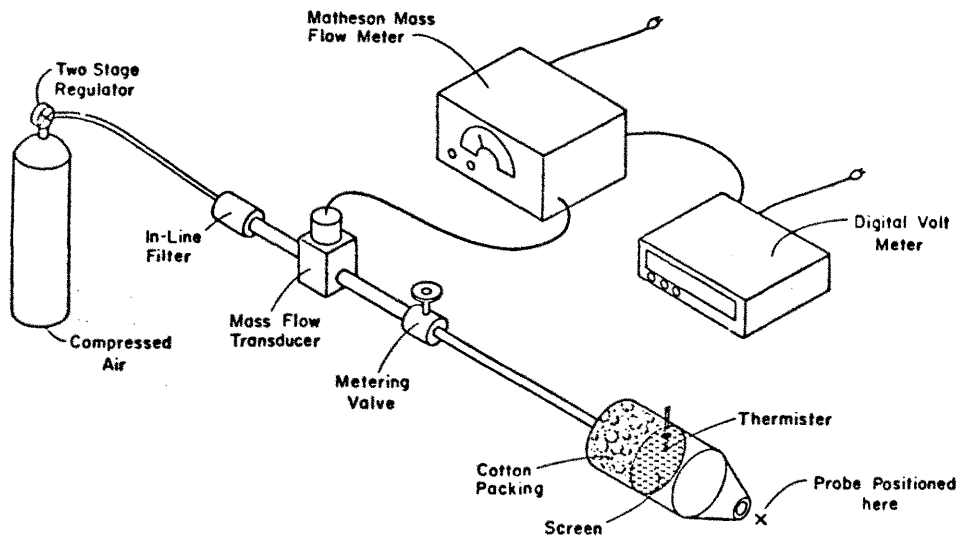
3.4 WIND PROFILE AND TURBULENCE MEASUREMENTS

The velocity profile, reference wind speed conditions, and turbulence were measured with a Thermo-Systems Inc. (TSI) 1050 anemometer and a TSI model 1210 hot-film probe. Since the voltage response of these anemometers is nonlinear with respect to velocity, a multi-point calibration of system response versus velocity was utilized for data reduction.

The velocity standard was that depicted in Figure 6. This consisted of a Matheson model 8116-0154 mass flowmeter, a Yellowsprings thermistor, and a profile conditioning section constructed by the Engineering Research Center shop. The mass flowmeter measures mass flow rate independent of temperature and pressure, the thermistor measures the temperature at the exit conditions. The profile conditioning section forms a flat velocity profile of very low turbulence at the position where the probe is to be located. Incorporating a measurement of the ambient atmospheric pressure and a profile correction factor permits the calibration of velocity at the measurement station from 0.1-2.0 m/s.

During calibration of the single film anemometer, the anemometer voltage response values over the velocity range of interest were fit to an expression similar to that of King's law [26] but with a variable exponent. The accuracy of this technique is approximately ± 2 percent of the actual longitudinal velocity.

The velocity sensors were mounted on a vertical traverse and positioned over the measurement location on the model. The anemometer responses were fed to a Preston analog-to-digital converter and then directly to a HP-1000 minicomputer for immediate interpretation. The HP-1000 computer also controls probe position. A flow chart depicting the control sequence for this process is presented in Figure 7.



TSI Single Film Sensor

Figure 6. Velocity Probes and Velocity Standard

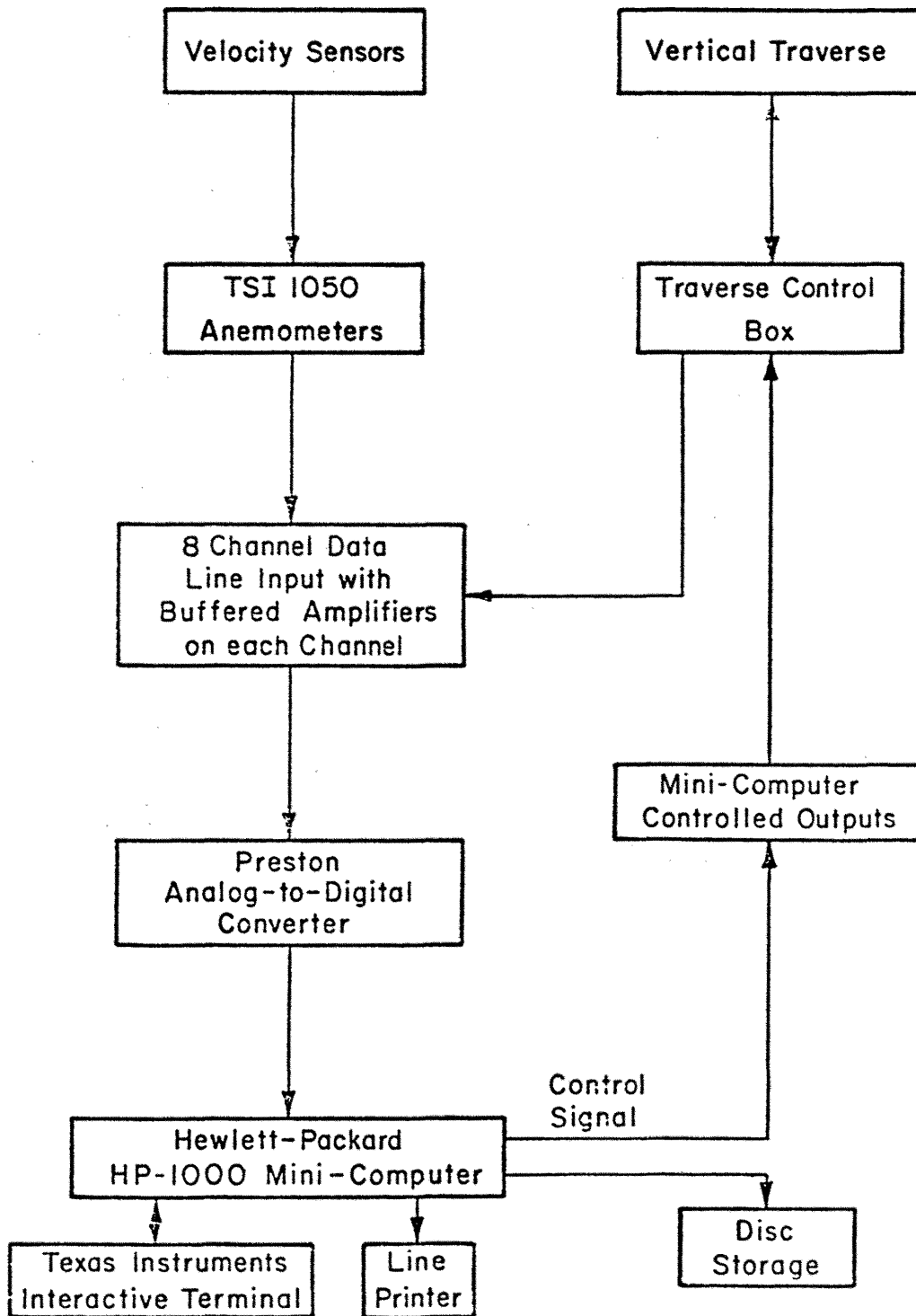


Figure 7. Velocity Data Reduction Flowchart

3.5 CONCENTRATION MEASUREMENTS

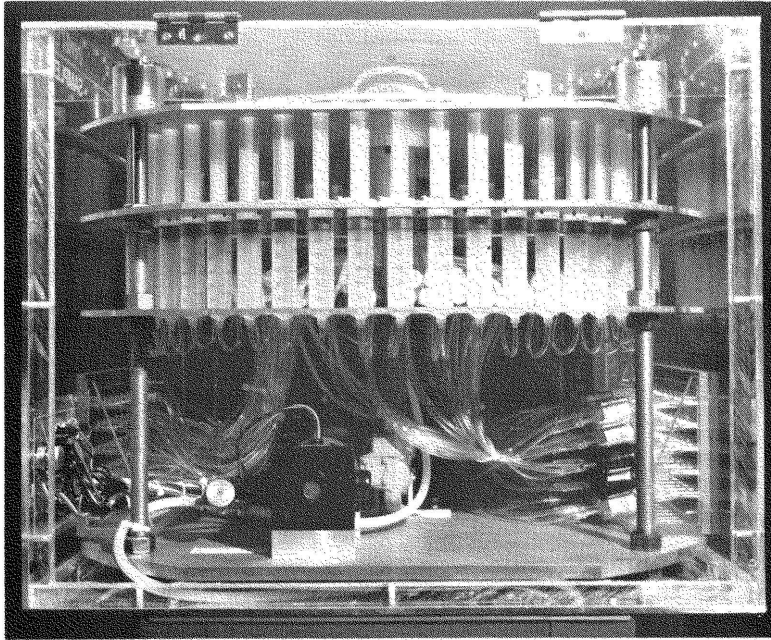
The experimental measurements of concentration were performed using gas-chromatograph and sampling systems (Figure 8) designed by Fluid Dynamics and Diffusion Laboratory staff.

3.5.1 Gas Chromatograph

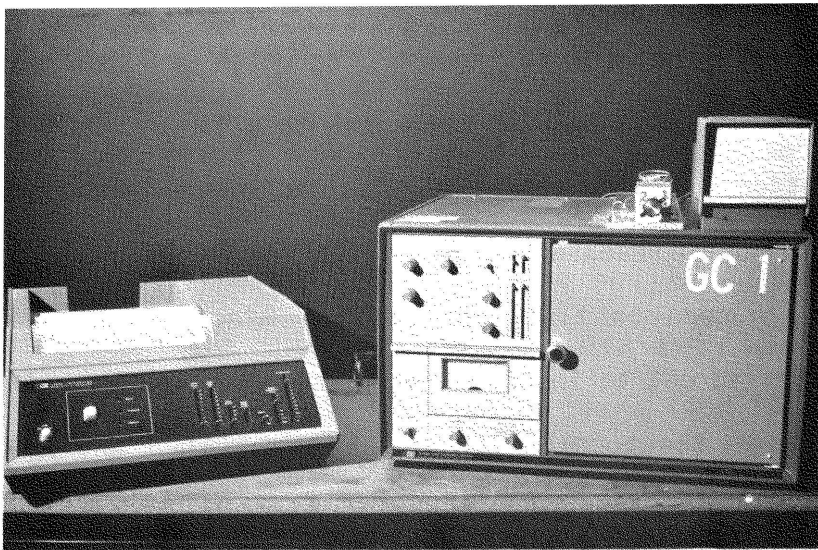
The gas chromatograph with Flame Ionization Detector (FID) operates on the principle that the electrical conductivity of a gas is directly proportional to the concentration of charged particles within the gas. The ions in this case are formed by the effluent gas being mixed in the FID with hydrogen and then burned in air. The ions and electrons formed enter an electrode gap and decrease the gap resistance. The resulting voltage drop is amplified by an electrometer and fed to the HP 3380 integrator. When no effluent gas is flowing, a carrier gas (nitrogen) flows through the FID. Due to certain impurities in the carrier, some ions and electrons are formed creating a background voltage or zero shift. When the effluent gas enters the FID, the voltage increase above this zero shift is proportional to the degree of ionization or correspondingly the amount of tracer gas present. Since the chromatograph¹ used in this study features a temperature control on the flame and electrometer, there is very low zero drift. In case of any zero drift, the HP 3380, which integrates the effluent peak, also subtracts out the zero drift.

The lower limit of measurement is imposed by the instrument sensitivity and the background concentration of tracer within the air in

¹A Hewlett Packard 5700 gas chromatograph was used in this study (shown in Figure 6).



(a)



(b)

Figure 8. Photographs of (a) the Gas Sampling System, and (b) the HP Integrator and Chromatograph

the wind tunnel. Background concentrations were measured and subtracted from all data quoted herein.

3.5.2 Sampling System

The tracer gas sampling system consists of a series of fifty 30 cc syringes mounted between two circular aluminum plates. A variable-speed motor raises a third plate, which in turn raises all 50 syringes simultaneously. A set of check valves and tubing are connected such that airflow from each tunnel sampling point passes over the top of each designated syringe. When the syringe plunger is raised, a sample from the tunnel is drawn into the syringe container. The sampling procedure consists of flushing (taking and expending a sample) the syringe three times after which the test sample is taken. The draw rate is variable and generally set to be approximately 6 cc/min.

The sampler was periodically calibrated to insure proper function of each of the check valve and tubing assemblies. The sampler intake was connected to short sections of Tygon tubing which led to a sampling manifold. The manifold, in turn, was connected to a gas cylinder having a known concentration of tracer gas. The gas was turned on and a valve on the manifold opened to release the pressure produced in the manifold. The manifold was allowed to flush for about 1 min. Normal sampling procedures were carried out to insure exactly the same procedure as when taking a sample from the tunnel. Each sample was then analyzed for tracer gas concentration. Any sample having an error of greater than ± 2 percent indicated a failure in the check valve assembly and the check valve was replaced or the bed syringe was not used for sampling from the tunnel.

3.5.3 Test Procedure

The test procedure consisted of: 1) setting the proper tunnel wind speed, 2) releasing a metered mixture of source gas (specific gravity of 1.5) from the release area source, 3) withdrawing samples of air from the tunnel at the locations designated, and 4) analyzing the samples with a Flame Ionization Gas Chromatograph (FIGC). Photographs of the sampling system and gas chromatograph are shown in Figure 8. The samples were drawn into each syringe over a 300 s (approximate) time period and consecutively injected into the FIGC.

The procedure for analyzing air samples from the tunnel is as follows: 1) a 2 cc sample volume which was drawn from the wind tunnel and collected in syringe is introduced into the Flame Ionization Detector (FID), 2) the output from the electrometer (in microvolts) is sent to the Hewlett-Packard 3380 Integrator, 3) the output signal is analyzed by the HP 3380 to obtain the proportional amount of hydrocarbons present in the sample, 4) the record is integrated, and the ethane concentration is determined by multiplying the integrated signal ($\mu\text{v}\cdot\text{s}$) by a calibration factor ($\text{ppm}/\mu\text{v}\cdot\text{s}$), 5) a summary of the integrator analysis (gas retention time and integrated area ($\mu\text{v}\cdot\text{s}$)) is printed out on the integrator at the wind tunnel, 6) the integrated values and associated run information were tabulated on a specially designed form, 7) the integrated values for each tracer are entered into a computer along with pertinent run parameters, and 8) the computer program converts the raw data into mean concentration. The calibration factor was obtained by introducing a known quantity, χ_s , of tracer into the FIGC and recording the integrated value, I , in $\mu\text{v}\cdot\text{s}$.

The calibration factor is $\frac{\chi_s (\text{ppm})}{I (\mu\text{v-s})}$

Calibrations were obtained at the beginning and end of each measurement period.

4.0 TEST PROGRAM

The goals of the test series were to determine the effects of fences and vortex generators near the source on the dispersion of LNG plume. It is obvious that if one permits variation in source strength, rate of spill, mean flow velocity, fence and vortex generator size, and geometry of separation an almost infinite matrix of tests is possible. However, after discussions with GRI personnel the following test matrix was performed:

1. Continuous LNG spill rates of 20, 30, 40 m³/min to produce a significant density dominated dispersion region,
2. Four wind speeds, 4, 7, 9 and 12 m/sec at 10 m equivalent height, for fence data and three wind speeds, 4, 7 and 9 m/sec at 10 m equivalent height, for vortex generator data,
3. Fences and vortex generators of the sizes: 75x75x5 m, 150x150x5 m, 75x75x10 m, and 150x150x10 m,
4. LNG boiloff area with diameter of 75 m.

The coordinate system and sampling point locations used throughout this report along with configuration 0 identification, which had no fence or vortex generator, are given in Figure 9. It should be noted that all concentration measurements were performed at ground-level. Because of the expected symmetry of the concentration pattern, the sample points were placed only on negative y coordinates. A summary of the test program identifying run numbers, prototype wind speeds, various configuration numbers, fence and vortex generator heights, and LNG boiloff rates is given in Tables 1 and 2. The configurations 1 to 3 and 4 to 6 are described in Figures 10 and 11, respectively. The total program required 138 runs in the Environmental Wind Tunnel. The following formulae were utilized to convert field values to model values,

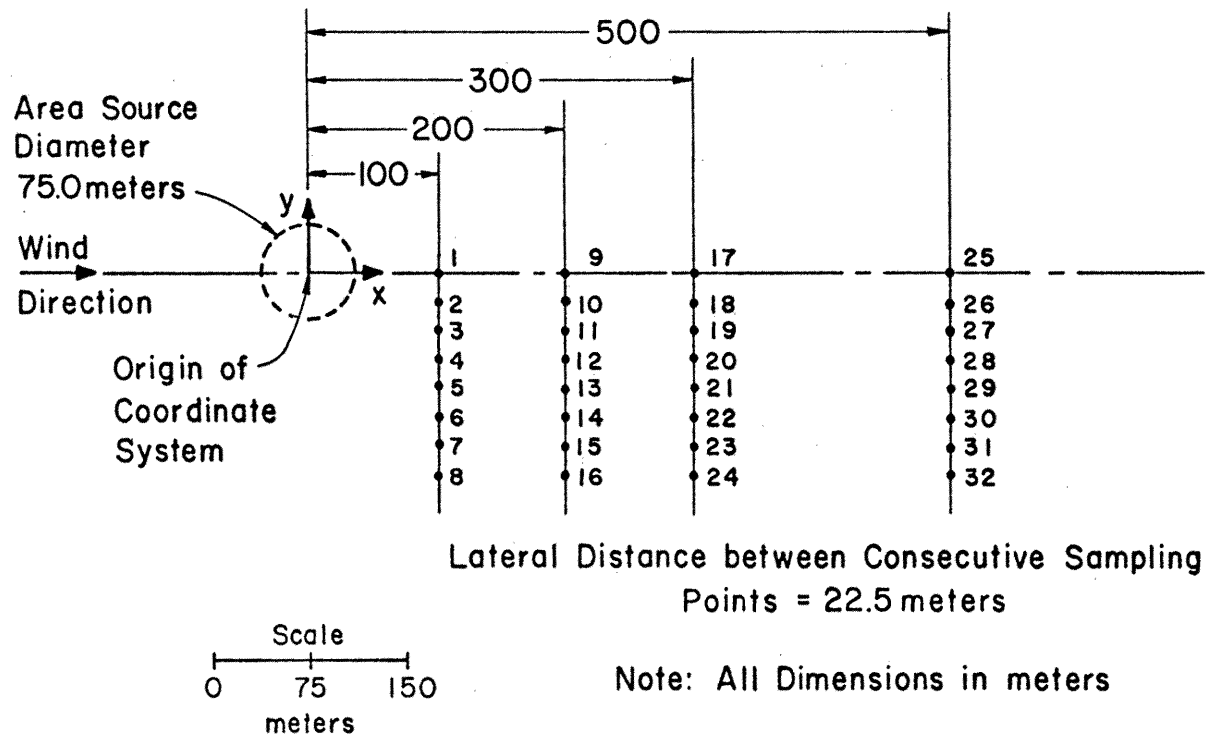


Figure 9. Concentration Measurement Locations and Configuration 0 Identification

Table 1. Summary of Tests (fence data)

Fence Height (m)	Fence Configuration Number	LNG Boiloff Rate (m ³ /min)	Wind Speed at 10 m (m/sec)	Run Number	Wind Speed at 10 m (m/sec)	Run Number	Wind Speed at 10 m (m/sec)	Run Number	Wind Speed at 10 m (m/sec)	Run Number
0	0	20	4	73	7	1	9	4	12	7
0	0	30	4	74	7	2	9	5	12	8
0	0	40	4	75	7	3	9	6	12	9
5	1	20	4	76	7	10	9	34	12	52
5	2	20	4	77	7	11	9	35	12	53
5	3	20	4	78	7	12	9	36	12	54
10	1	20	4	88	7	22	9	37	12	55
10	2	20	4	89	7	23	9	38	12	56
10	3	20	4	90	7	24	9	39	12	57
5	1	30	4	91	7	18	9	40	12	58
5	2	30	4	92	7	19	9	41	12	59
5	3	30	4	93	7	20	9	42	12	60
10	1	30	4	79	7	14	9	43	12	61
10	2	30	4	80	7	15	9	44	12	62
10	3	30	4	81	7	16	9	45	12	63
5	1	40	4	82	7	26	9	46	12	64
5	2	40	4	83	7	27	9	47	12	65
5	3	40	4	84	7	28	9	48	12	66
10	1	40	4	85	7	30	9	49	12	67
10	2	40	4	86	7	31	9	50	12	68
10	3	40	4	87	7	32	9	51	12	69

Table 2. Summary of Tests (vortex generator data)

Fence Height (m)	Fence Configuration Number	LNG Boiloff Rate (m ³ /min)	Wind Speed at 10 m (m/sec)	Run Number	Wind Speed at 10 m (m/sec)	Run Number	Wind Speed at 10 m (m/sec)	Run Number
5	4	20	4	151	7	169	9	187
5	5	20	4	152	7	170	9	188
5	6	20	4	153	7	171	9	189
10	4	20	4	160	7	178	9	196
10	5	20	4	161	7	179	9	197
10	6	20	4	162	7	180	9	198
5	4	30	4	154	7	172	9	190
5	5	30	4	155	7	173	9	191
5	6	30	4	156	7	174	9	192
10	4	30	4	163	7	181	9	199
10	5	30	4	164	7	182	9	200
10	6	30	4	165	7	183	9	201
5	4	40	4	157	7	175	9	193
5	5	40	4	158	7	176	9	194
5	6	40	4	159	7	177	9	195
10	4	40	4	166	7	184	9	202
10	5	40	4	167	7	185	9	203
10	6	40	4	168	7	186	9	204

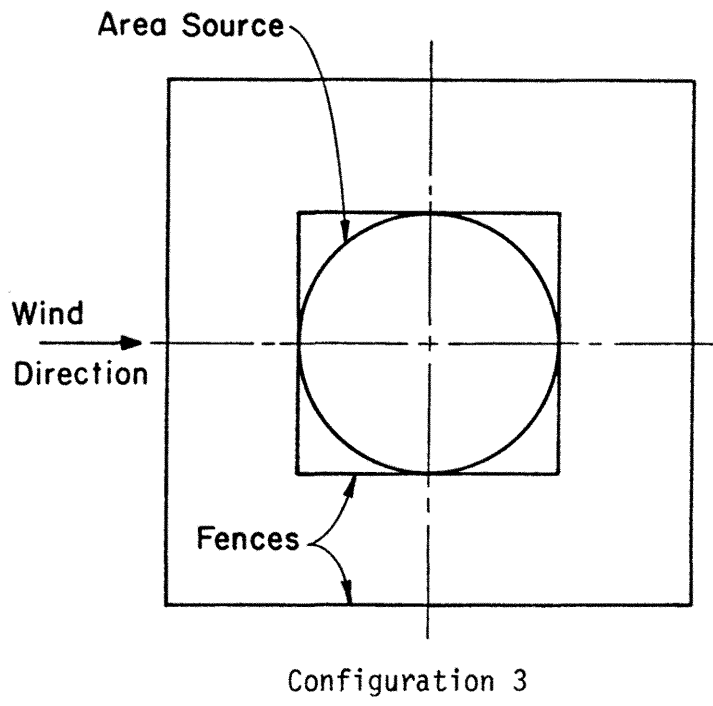
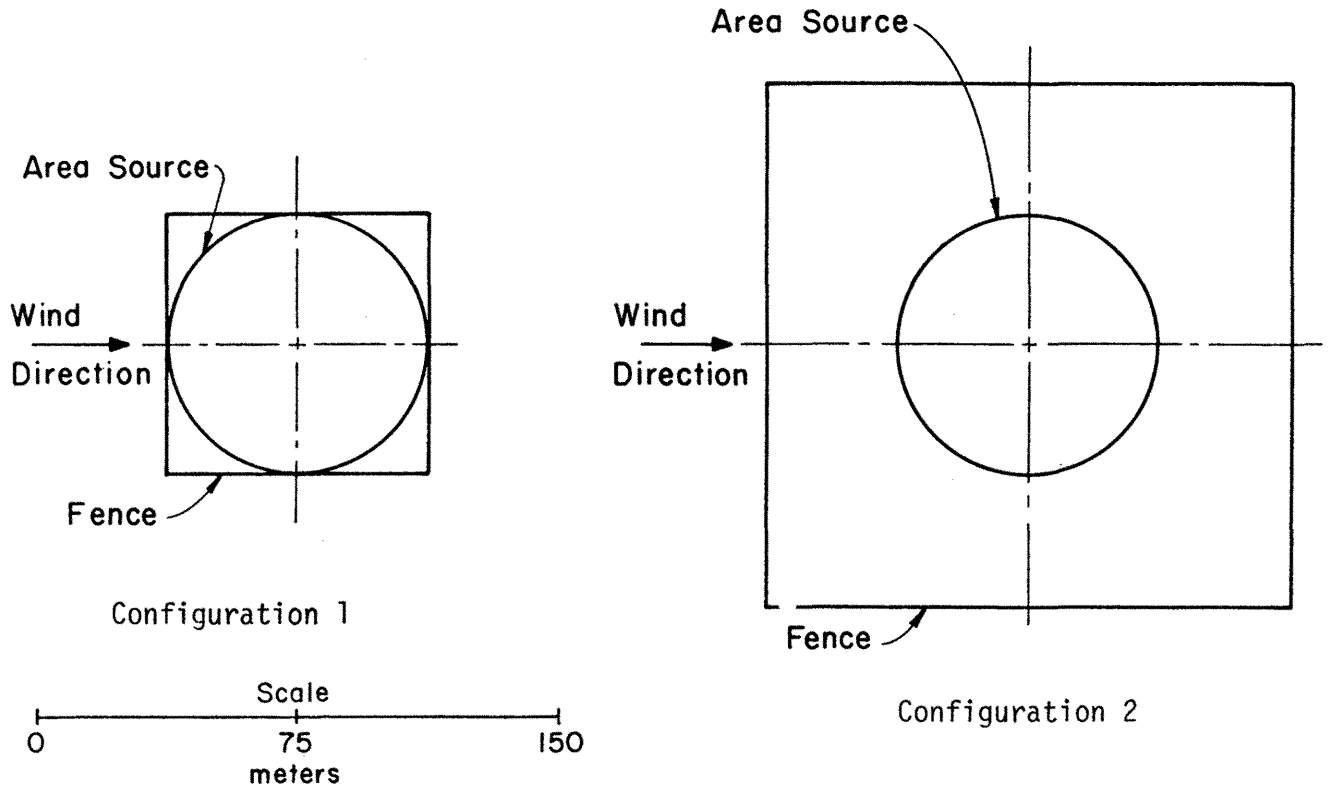


Figure 10. Configurations 1 to 3 Identification

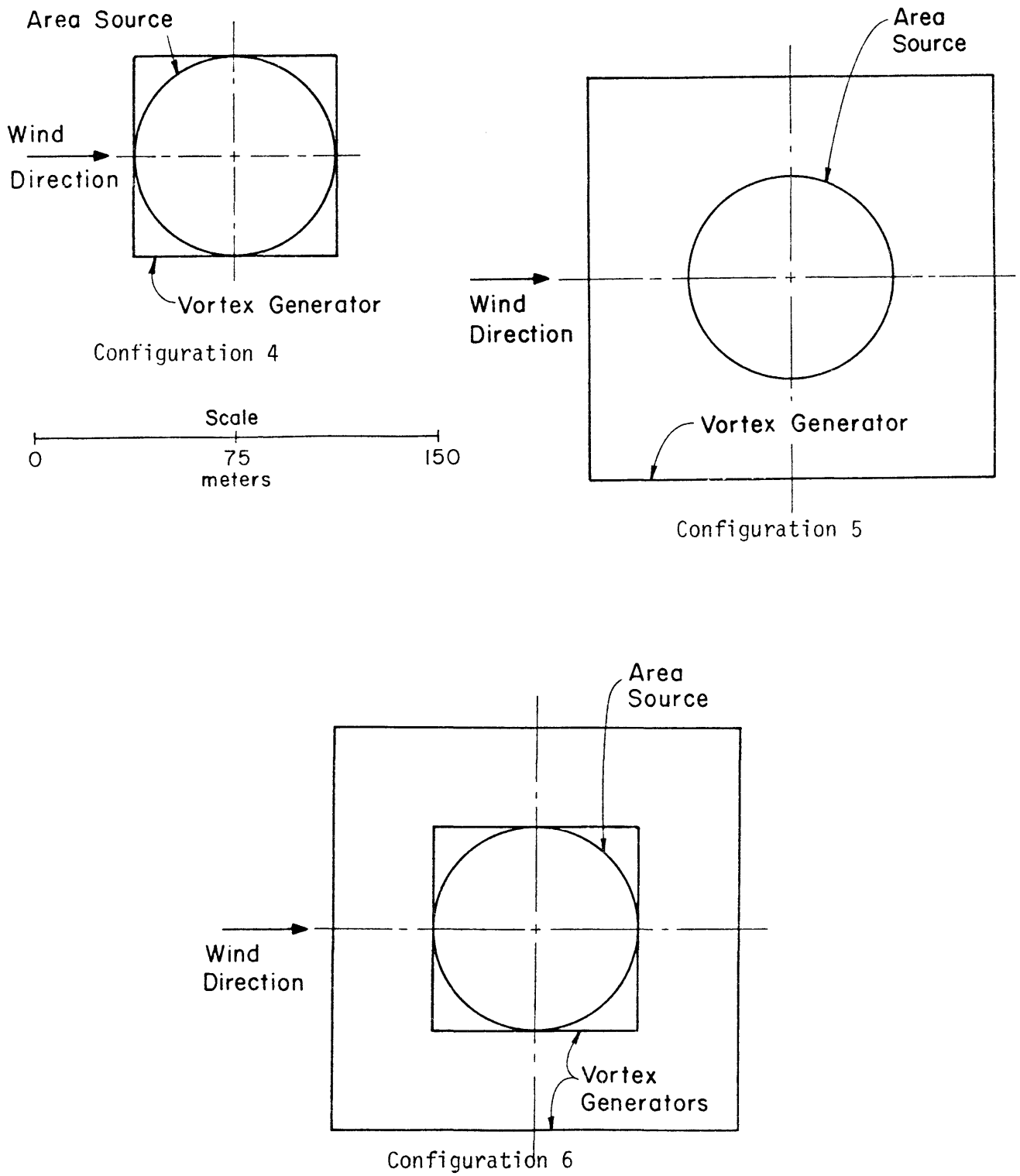


Figure 11. Configurations 4 to 6 Identification

$$L_m = \frac{1}{L.S.} L_p ,$$

with LNG plume,

$$U_m = \left(\frac{S.G._m - 1}{S.G._p - 1} \right)^{1/2} \left(\frac{L_m}{L_p} \right)^{1/2} U_p ,$$

$$Q_m = \left(\frac{S.G._m - 1}{S.G._p - 1} \right)^{1/2} \left(\frac{L_m}{L_p} \right)^{5/2} Q_p ,$$

where,

L is length,

U is reference wind speed at 10 m height,

Q is plume flow rate at the source,

L.S. is length scale factor (250),

S.G. is plume specific gravity at the source, and
subscripts m and p indicate model and prototype (field)
conditions, respectively.

4.1 RESULTS AND DISCUSSION

4.1.1 Approach Velocities

The approach flow velocity profiles were measured at the location of the area source center. The characteristic mean velocity and turbulence profiles are displayed in Figures 12 through 15. The average value of the velocity profile power-law exponent was 0.16. The values of the frictional velocity, u_* , were 0.23, 0.42, 0.5, 0.66 m/sec corresponding to prototype wind speeds of 4, 7, 9 and 12 m/sec at 10 m height. The average value of the surface roughness parameter, z_0 for prototype conditions was 3.8 cm.

4.1.2 Flow Visualization Results

The various configurations with vortex generators or fences were installed in the wind tunnel and flow visualization was performed with

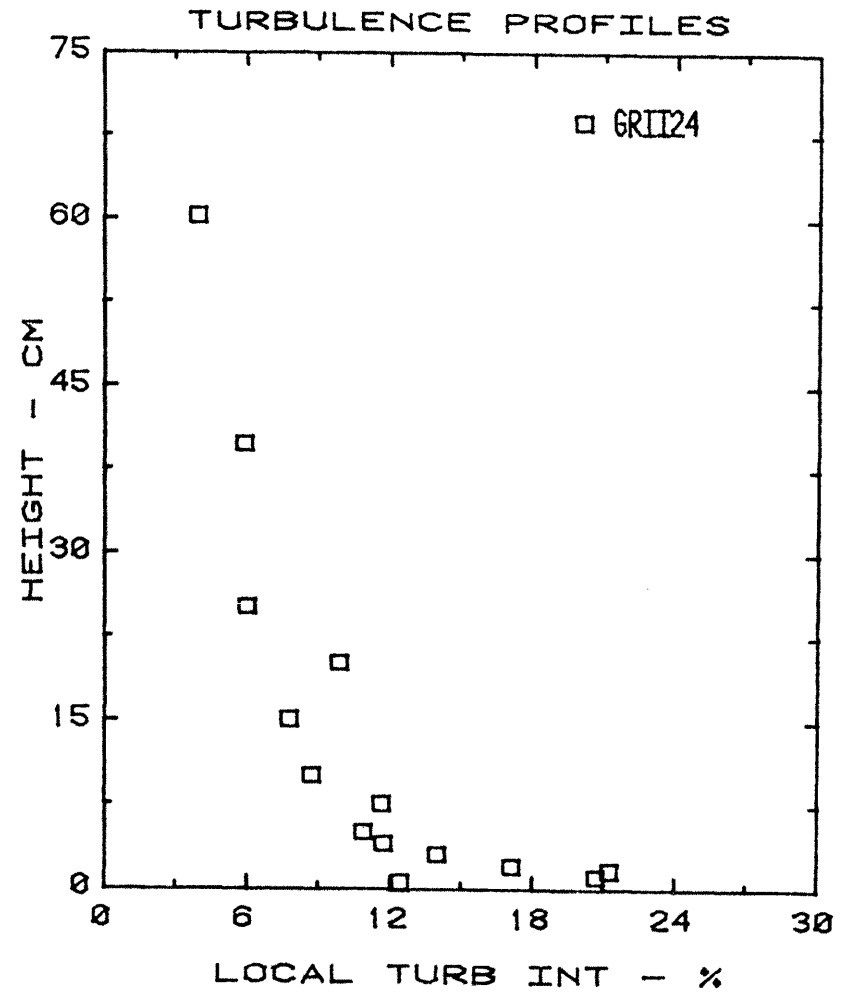
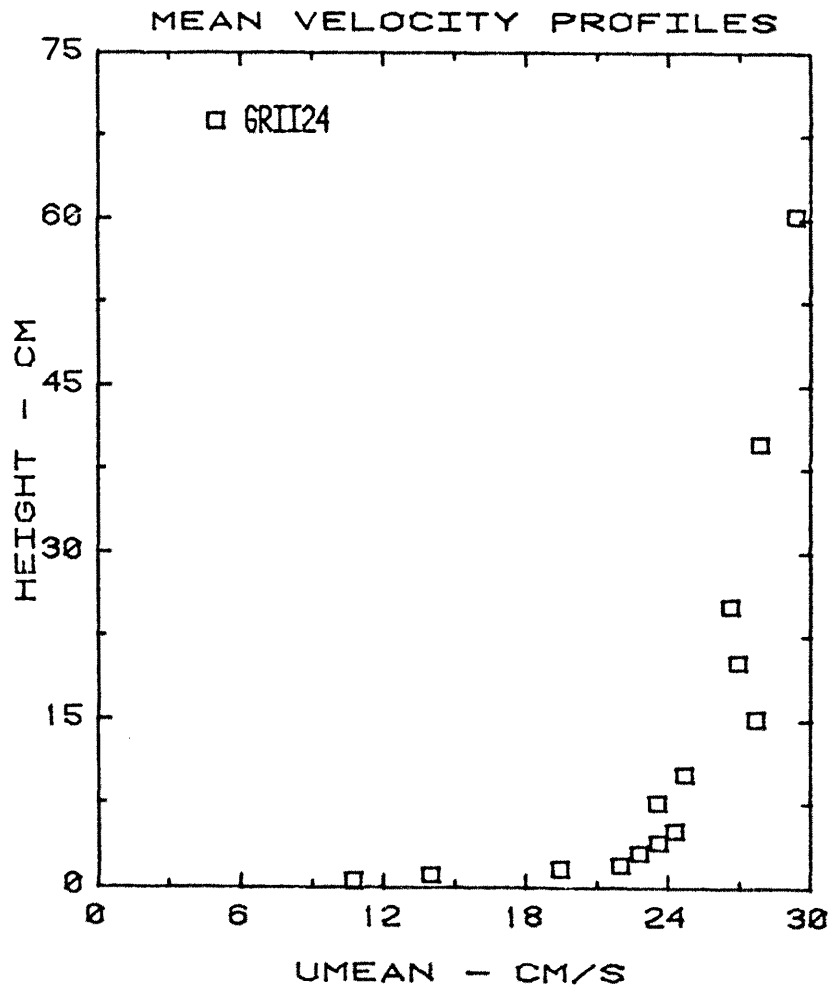


Figure 12. Mean Velocity and Turbulence Intensity Profiles for Equivalent Prototype
Wind Speed of 4 m/sec at 10 m Height

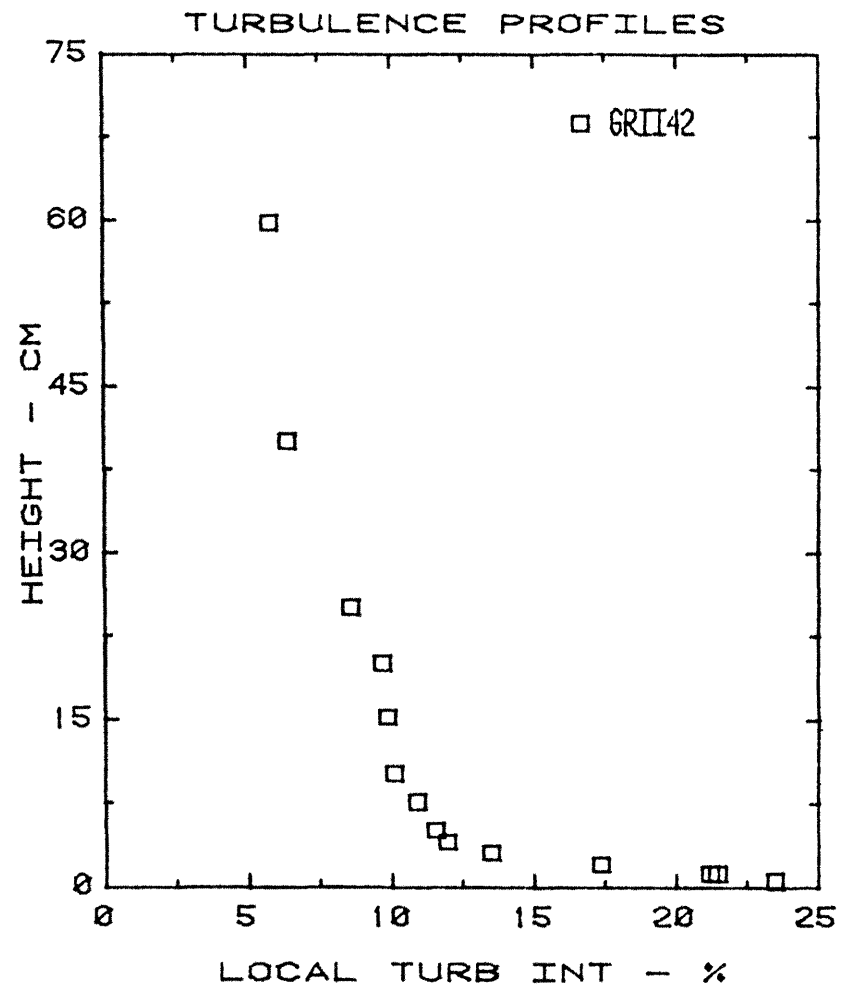
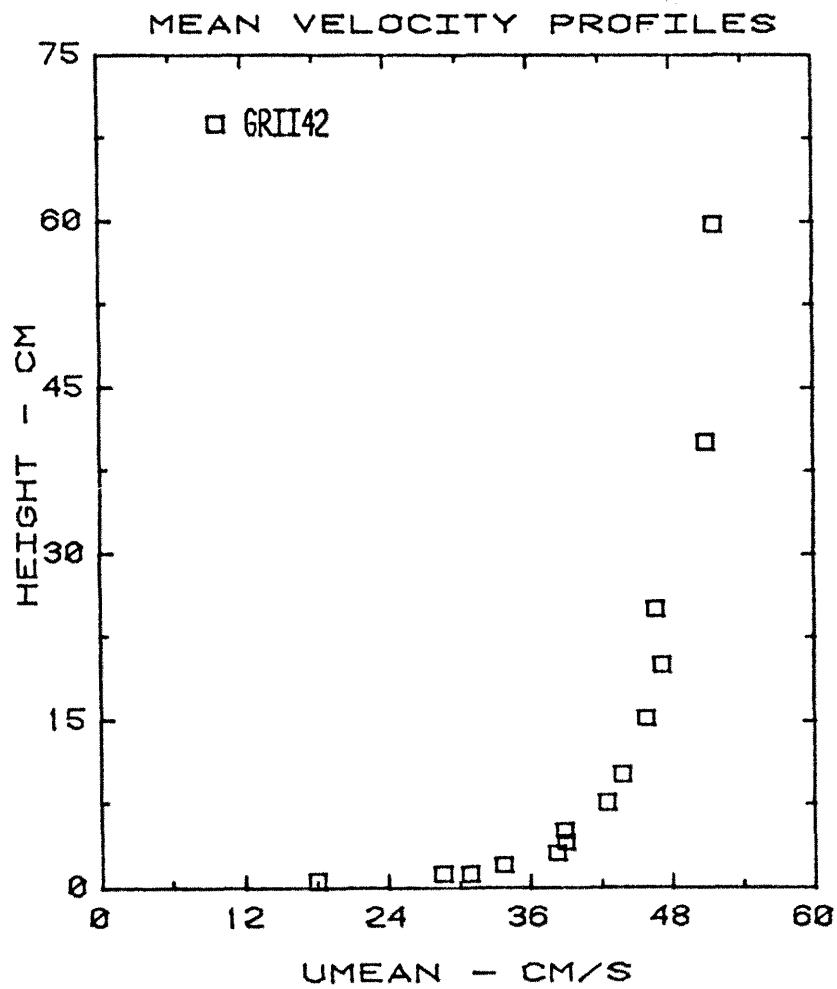


Figure 13. Mean Velocity and Turbulence Intensity Profiles for Equivalent Prototype Wind Speed of 7 m/sec at 10 m Height

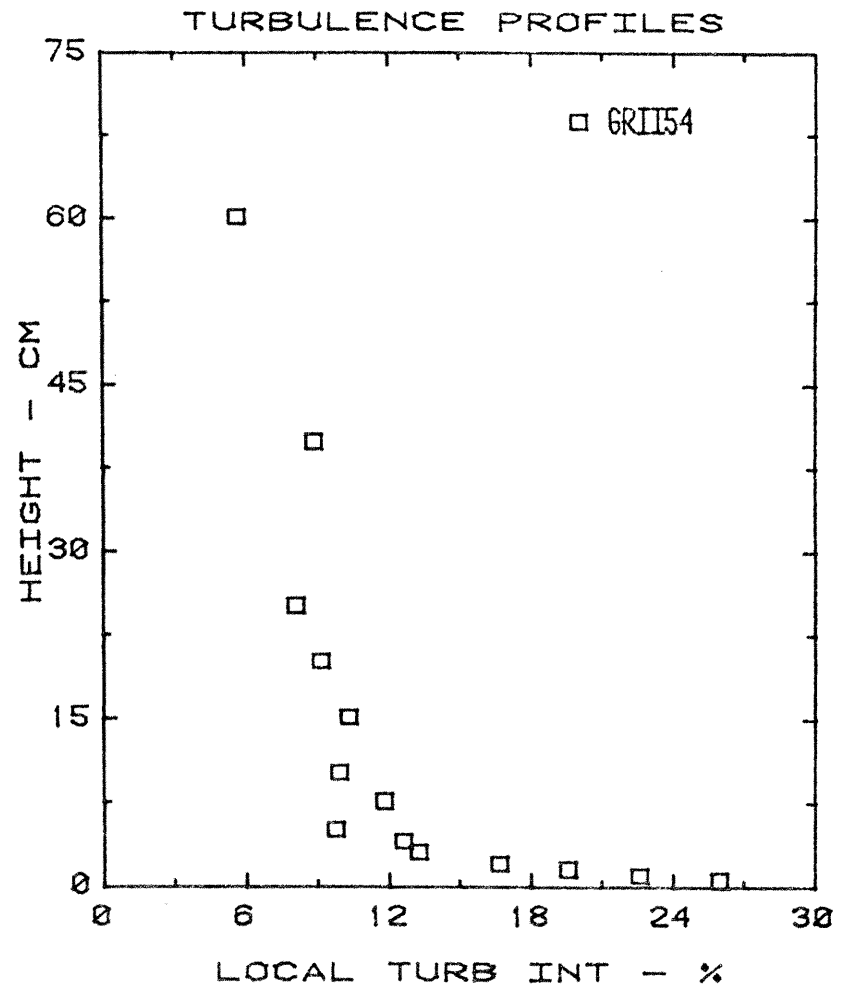
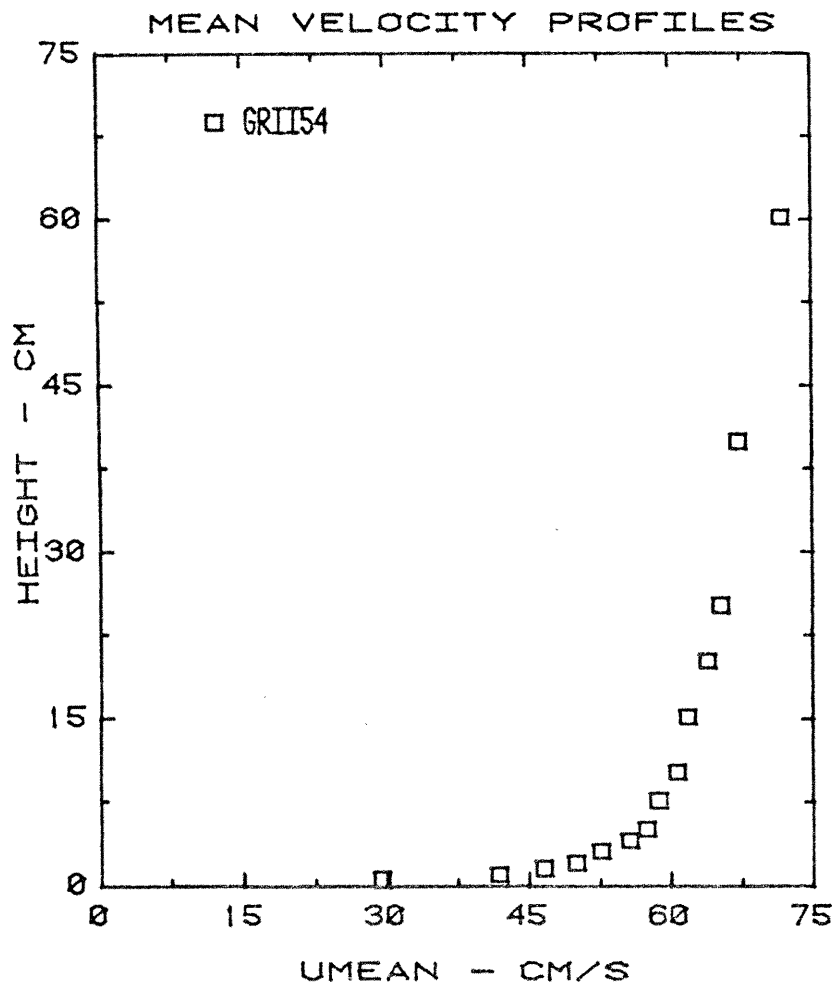


Figure 14. Mean Velocity and Turbulence Intensity Profiles for Equivalent Prototype Wind Speed of 9 m/sec at 10 m Height

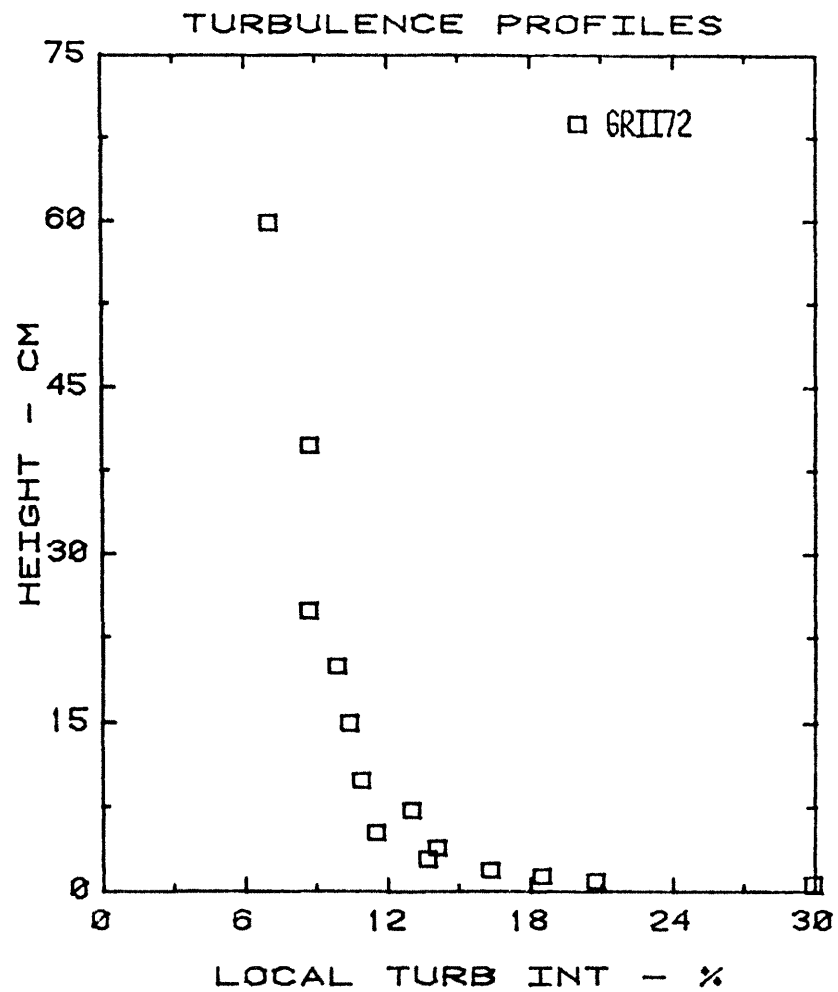
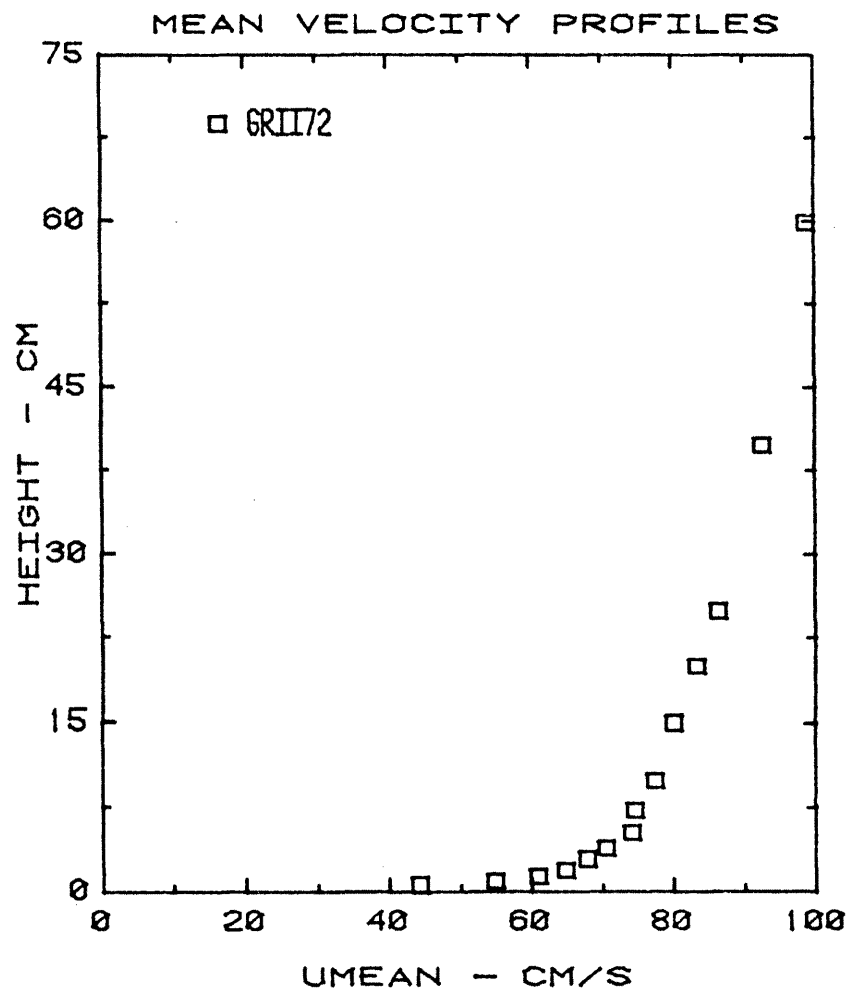


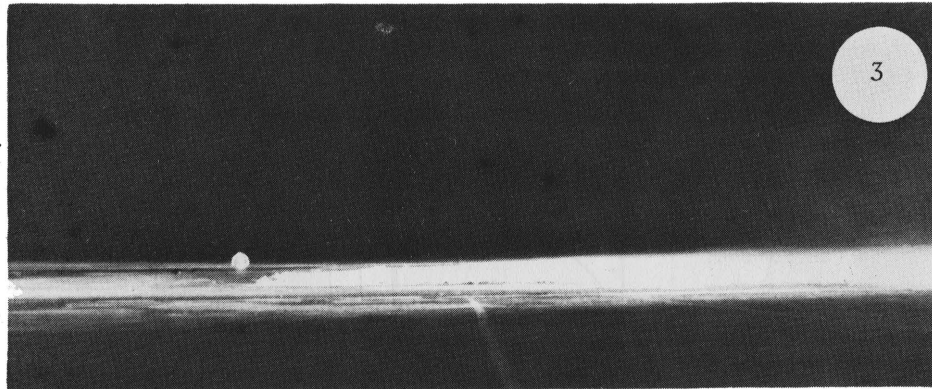
Figure 15. Mean Velocity and Turbulence Intensity Profiles for Equivalent Prototype Wind Speed of 12 m/sec at 10 m Height

40 m³/min LNG equivalent flow rate and three wind speeds. For each test, 4x5 black and white still photographs and 35 mm color slides were obtained to determine the plume geometry. The typical visualization photographs are shown in Figure 16 for run numbers 3, 30, and 184. It should be noted that fences and vortex generators create vertical mixing and result in plume spread in the vertical direction. This vertical mixing reduces the ground level concentrations hazards.

4.1.3 Concentration Measurement Results

All the concentration measurement results from 138 test runs are given in Appendix B. Many researchers have observed that for a ground base neutrally buoyant plume the concentrations decay versus longitudinal distance follows a straight line relationship when plotted on a log-log scale. Hence, in this study interpolation of the concentrations along the longitudinal direction were obtained with curve fit through logarithms of the data points at each of the lateral distances. However, the lateral interpolation of the concentration were obtained with curve fit through the concentration data itself at each longitudinal distances. The ground level concentration contour isopleths were plotted for all the runs. The experimental results presented here are to determine the effects of variations in: 1) LNG boiloff rates, 2) wind speeds, 3) fence or vortex generator configurations, 4) fence or vortex generator heights, and 5) the type of accelerated dilution device.

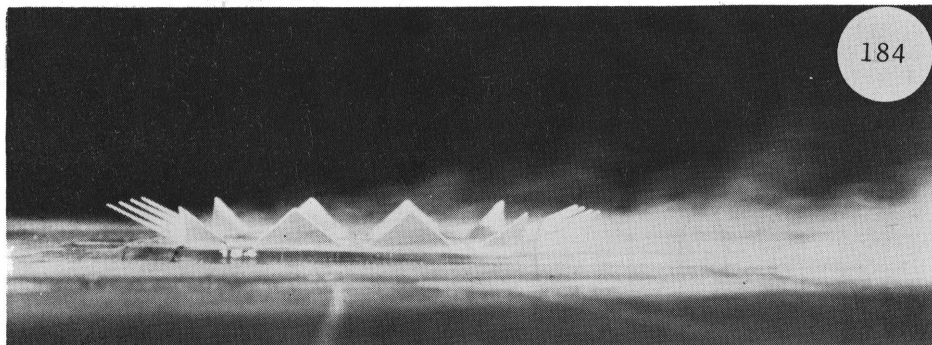
The results presented in the report are the representative of the various cases. Similar results were obtained for the cases not presented as concentration isopleths. Figures 17 through 39 present the plots of ground-level mean concentration isopleth contours for various



(a)



(b)



(c)

Figure 16. Flow visualization (a) No Fence or Vortex Generator; (b) 4 cm (10 m) Height Fence, Configuration 1; (c) 4 cm (10 m) Height Vortex Generator, Configuration 4; Equivalent Wind Speed 7 m/sec at 10 m Height, Equivalent LNG Boiloff rate of 40 m³/min

RUN NUMBER = 1 CØNFIGURATIØN = 0

MØDEL FLØW RATE = 4473.0 CC/MIN
PRØTØTYPE FLØW RATE = 20.0 (M) (M) (M) / MIN
MØDEL VELØCITY = .42 M/SEC AT 4 CM
PRØTØTYPE VELØCITY = 7.0 M/SEC AT 10 M
MØDEL FENCE HEIGHT = 0.0 CM
PRØTØTYPE FENCE HEIGHT = 0.0 M

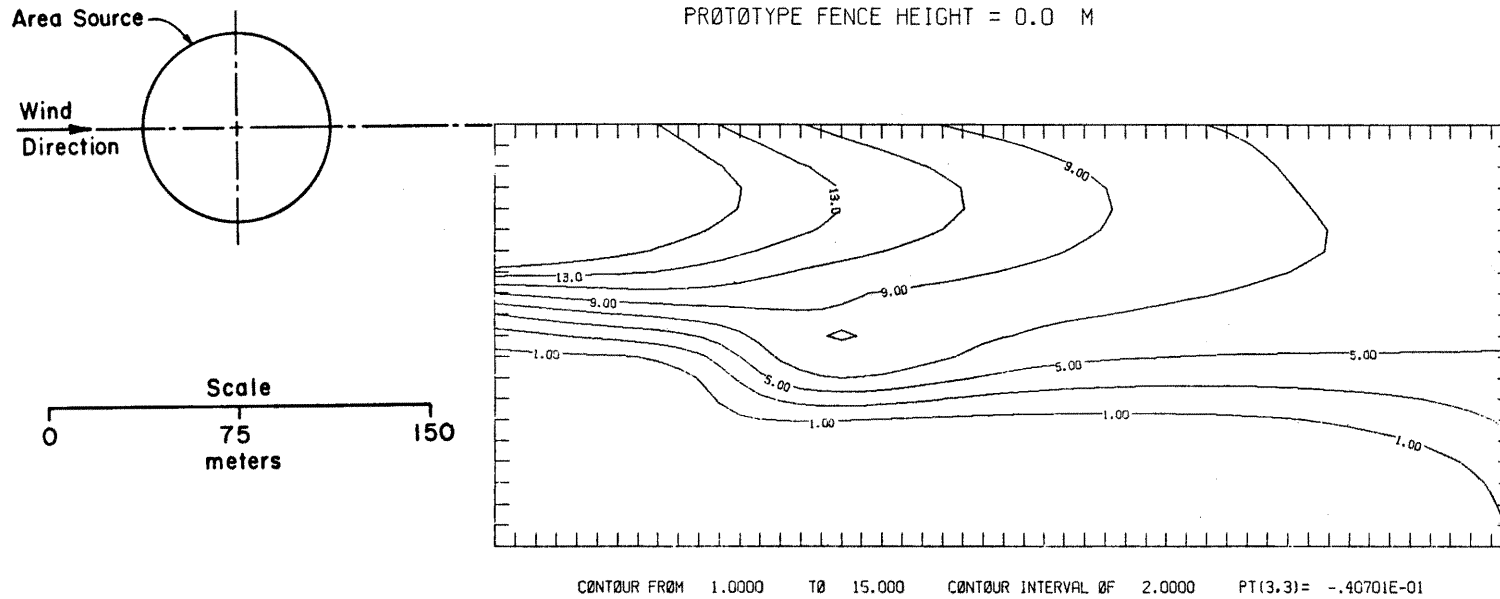


Figure 17. Ground-level Mean Concentration Isopleths for Run Number 1

RUN NUMBER = 2 CONFIGURATION = 0

MODEL FLOW RATE = 6710.0 CC/MIN
PROTOTYPE FLOW RATE = 30.0 (M) (M) (M) / MIN
MODEL VELOCITY = .42 M/SEC AT 4 CM
PROTOTYPE VELOCITY = 7.0 M/SEC AT 10 M
MODEL FENCE HEIGHT = 0.0 CM
PROTOTYPE FENCE HEIGHT = 0.0 M

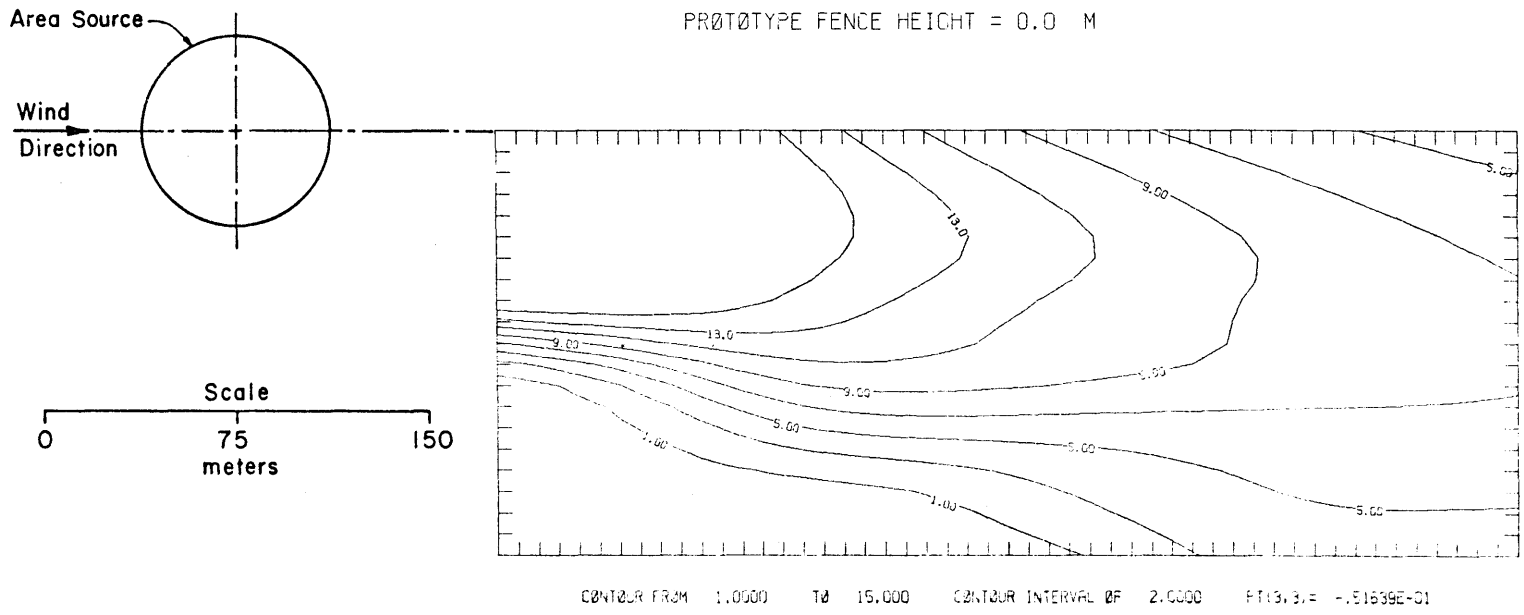


Figure 18. Ground-level Mean Concentration Isopleths for Run Number 2

RUN NUMBER = 3 CØNFIGURATION = 0

MØDEL FLØW RATE = 8946.0 CC/MIN
PRØTØTYPE FLØW RATE = 40.0 (M)(M)(M)/MIN
MØDEL VELOCITY = .42 M/SEC AT 4 CM
PRØTØTYPE VELOCITY = 7.0 M/SEC AT 10 M
MØDEL FENCE HEIGHT = 0.0 CM
PRØTØTYPE FENCE HEIGHT = 0.0 M

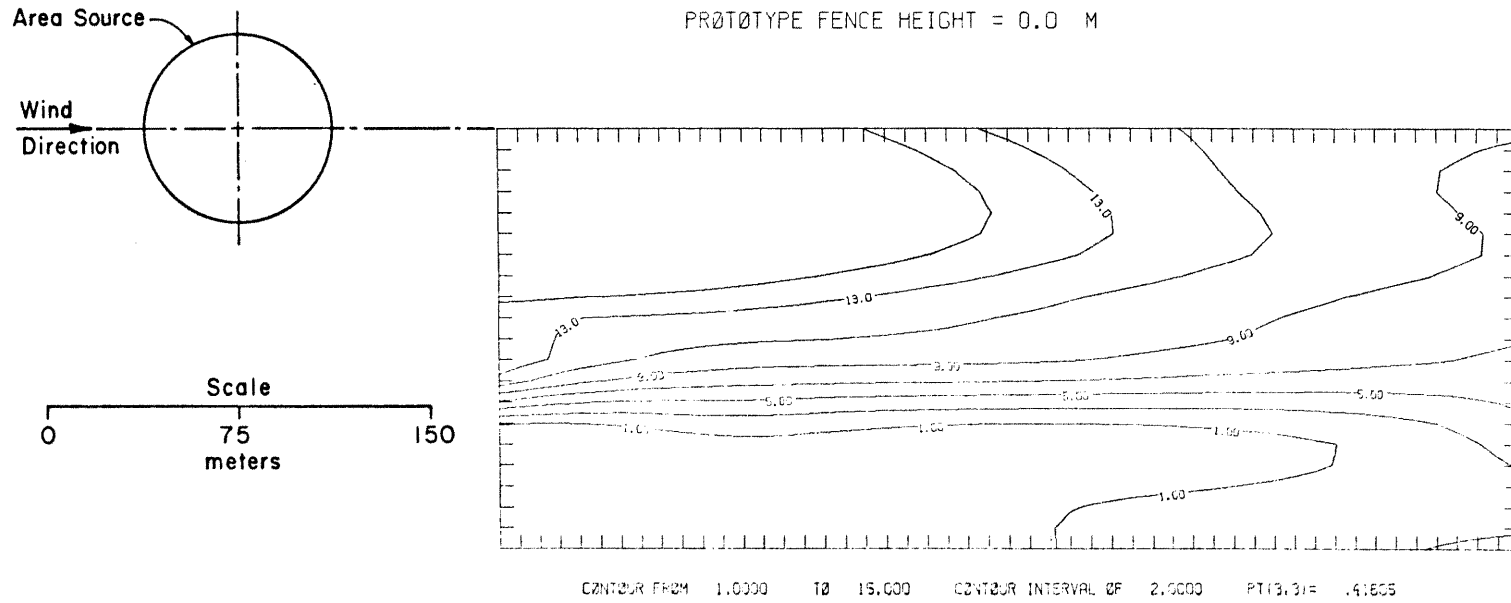


Figure 19. Ground-level Mean Concentration Isopleths for Run Number 3

RUN NUMBER = 5 CONFIGURATION = 0

MODEL FLOW RATE = 6710.0 CC/MIN
PROTOTYPE FLOW RATE = 30.0 (M)(M)(M)/MIN
MODEL VELOCITY = .54 M/SEC AT 4 CM
PROTOTYPE VELOCITY = 9.0 M/SEC AT 10 M
MODEL FENCE HEIGHT = 0.0 CM
PROTOTYPE FENCE HEIGHT = 0.0 M

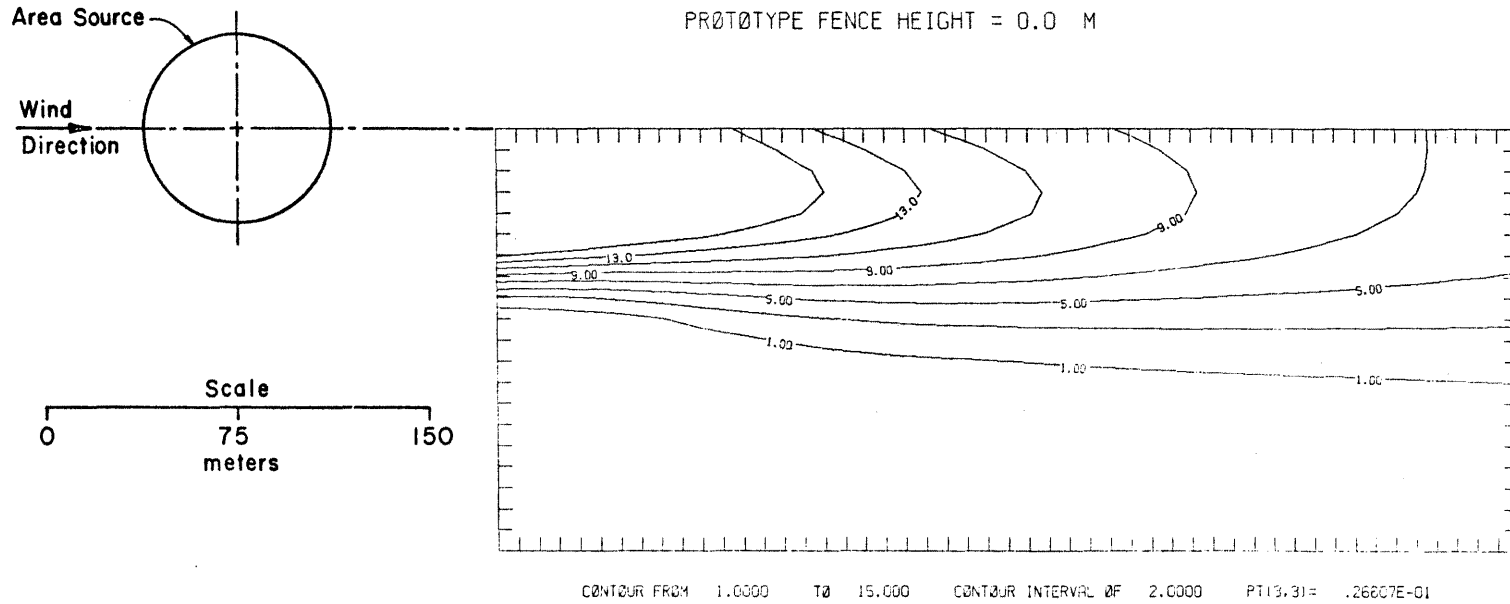


Figure 20. Ground-level Mean Concentration Isopleths for Run Number 5

RUN NUMBER = 8 CONFIGURATION = 0

MODEL FLOW RATE = 6710.0 CC/MIN
PROTOTYPE FLOW RATE = 30.0 (M)(M)(M)/MIN
MODEL VELOCITY = .72 M/SEC AT 4 CM
PROTOTYPE VELOCITY = 12.0 M/SEC AT 10 M
MODEL FENCE HEIGHT = 0.0 CM
PROTOTYPE FENCE HEIGHT = 0.0 M

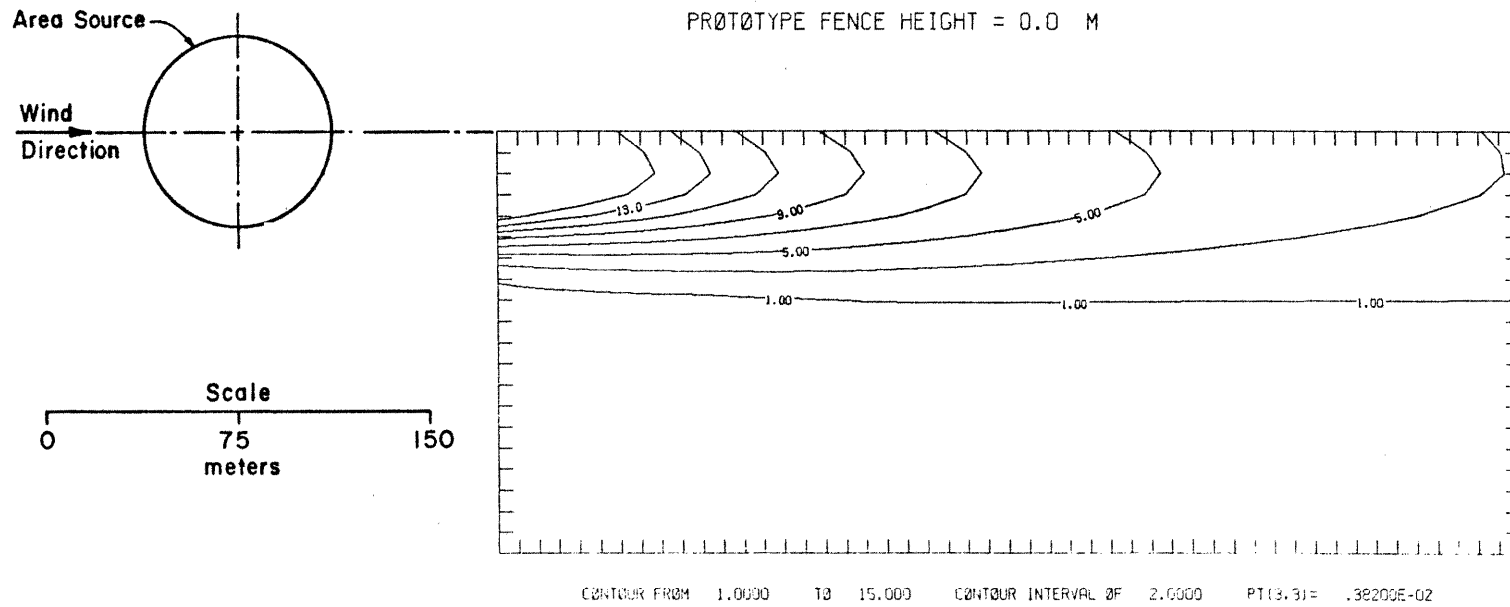
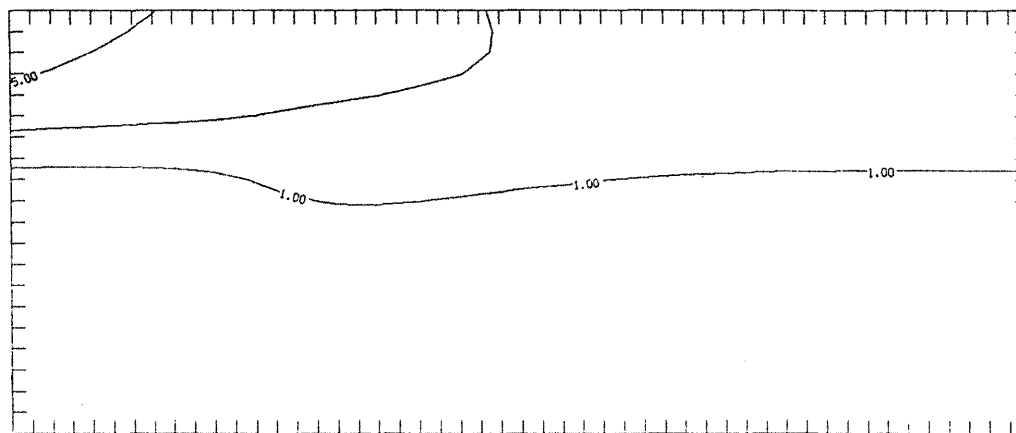
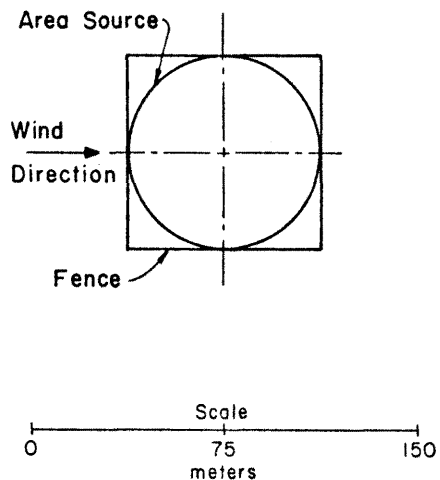


Figure 21. Ground-level Mean Concentration Isopleths for Run Number 8

RUN NUMBER = 10 CONFIGURATION = 1

MODEL FLOW RATE = 4473.0 CC/MIN
PROTOTYPE FLOW RATE = 20.0 (M)(M)(M)/MIN
MODEL VELOCITY = .42 M/SEC AT 4 CM
PROTOTYPE VELOCITY = 7.0 M/SEC AT 10 M
MODEL FENCE HEIGHT = 2.0 CM
PROTOTYPE FENCE HEIGHT = 5.0 M

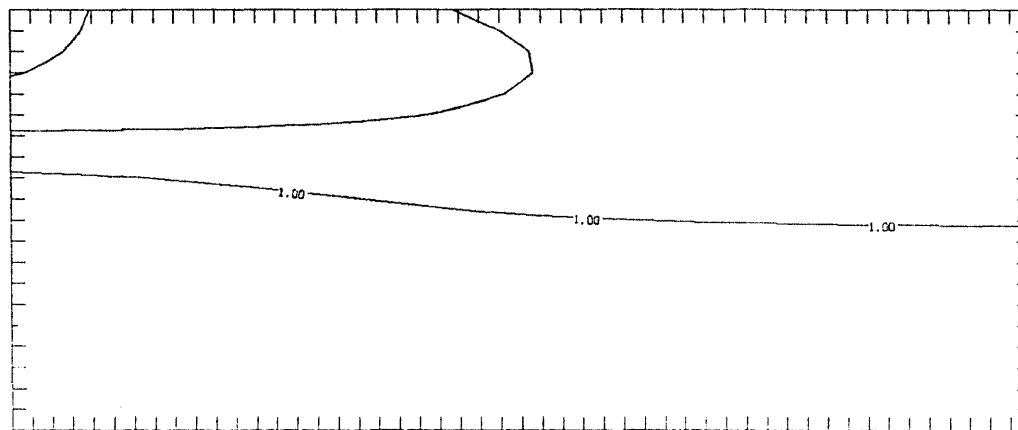
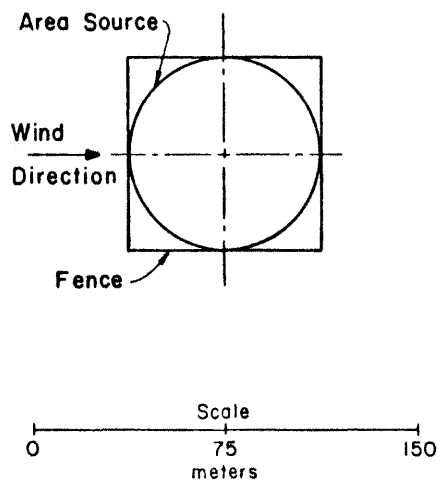


CONTOUR FROM 1.0000 TO 15.0000 CONTOUR INTERVAL OF 2.0000 PT(3,3) = .57017E-02

Figure 22. Ground-level Mean Concentration Isopleths for Run Number 10

RUN NUMBER = 14 CØNFIGURATIØN = 1

MØDEL FLØW RATE = 6710.0 CC/MIN
PRØTØTYPE FLØW RATE = 30.0 (M)(M)(M)/MIN
MØDEL VELØCITY = .42 M/SEC AT 4 CM
PRØTØTYPE VELØCITY = 7.0 M/SEC AT 10 M
MØDEL FENCE HEIGHT = 4.0 CM
PRØTØTYPE FENCE HEIGHT = 10.0 M

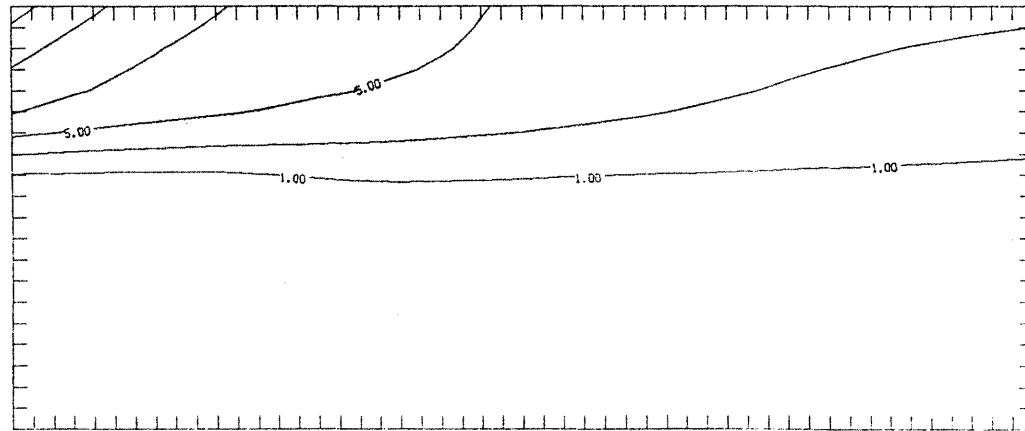
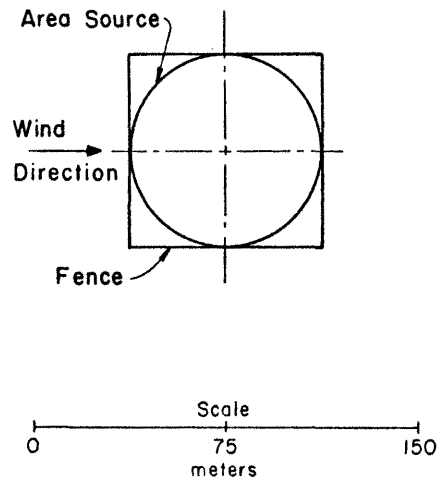


CØNTOUR FROM 1.0000 TO 15.0000 CØNTOUR INTERVAL OF 2.0000 FT(1.3)= .33320E-02

Figure 23. Ground-level Mean Concentration Isopleths for Run Number 14

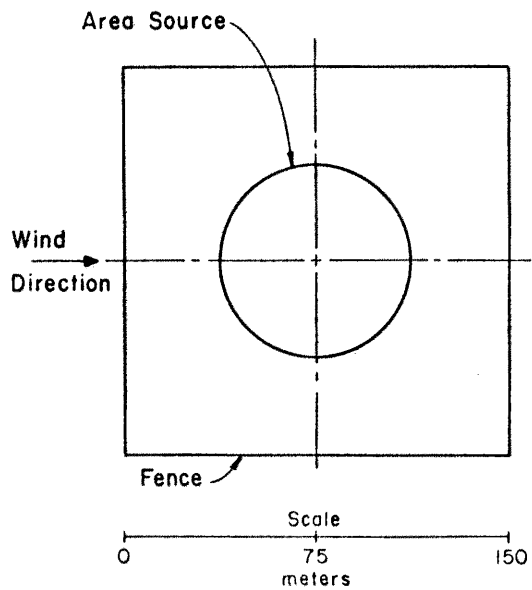
RUN NUMBER = 18 CONFIGURATION = 1

MODEL FLOW RATE = 6710.0 CC/MIN
PROTOTYPE FLOW RATE = 30.0 (M)(M)(M)/MIN
MODEL VELOCITY = .42 M/SEC AT 4 CM
PROTOTYPE VELOCITY = 7.0 M/SEC AT 10 M
MODEL FENCE HEIGHT = 2.0 CM
PROTOTYPE FENCE HEIGHT = 5.0 M



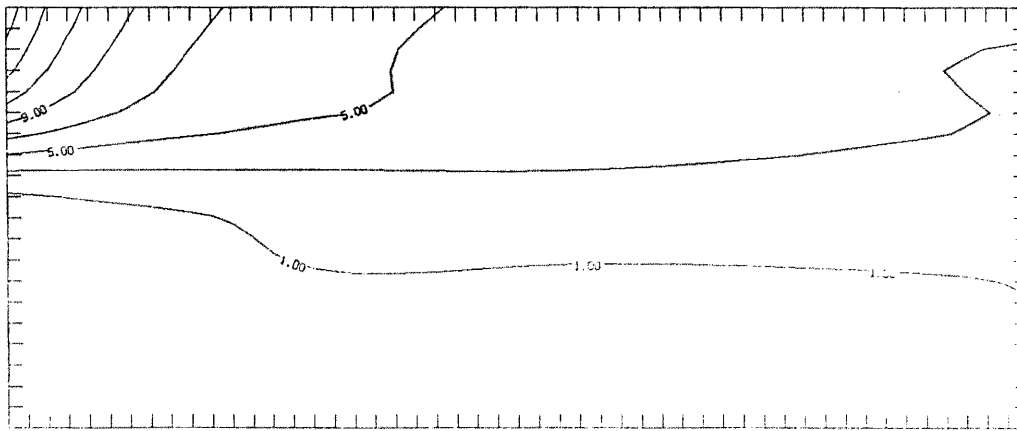
CONTOUR FROM 1.0000 TO 15.0000 CONTOUR INTERVAL OF 2.0000 PT(3,3) = .11885E-01

Figure 24. Ground-level Mean Concentration Isopleths for Run Number 18



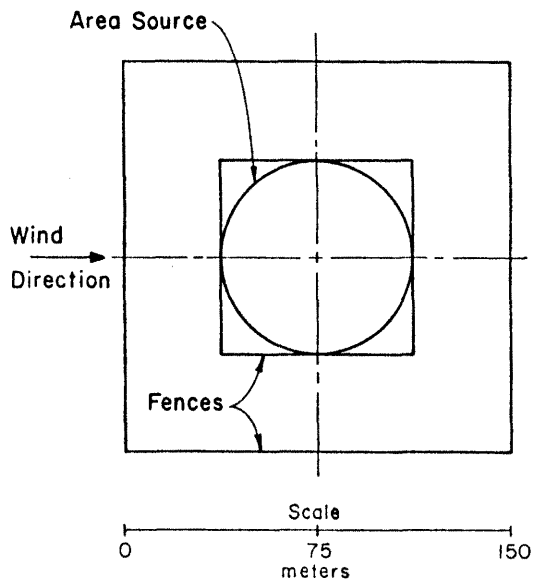
RUN NUMBER = 19 CONFIGURATION = 2

MODEL FLOW RATE = 6710.0 CC/MIN
 PROTOTYPE FLOW RATE = 30.0 (M)(M)(M)/MIN
 MODEL VELOCITY = .42 M/SEC AT 4 CM
 PROTOTYPE VELOCITY = 7.0 M/SEC AT 10 M
 MODEL FENCE HEIGHT = 2.0 CM
 PROTOTYPE FENCE HEIGHT = 5.0 M



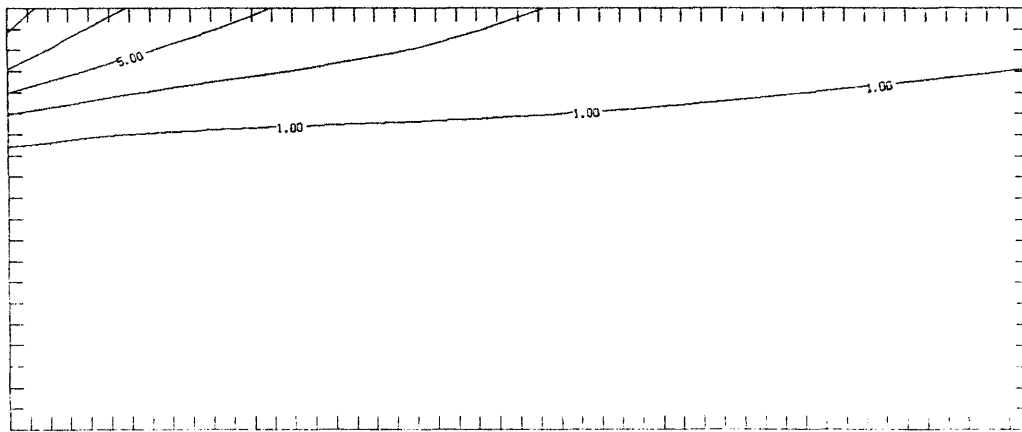
CONTOUR FROM 1.0000 TO 15.0000 CONTOUR INTERVAL OF 2.0000 PT(3,3)= -1.10590E-02

Figure 25. Ground-level Mean Concentration Isopleths for Run Number 19



RUN NUMBER = 20 CONFIGURATION = 3

MODEL FLOW RATE = 6710.0 CC/MIN
 PROTOTYPE FLOW RATE = 30.0 (M)(M)(M)/MIN
 MODEL VELOCITY = .42 M/SEC AT 4 CM
 PROTOTYPE VELOCITY = 7.0 M/SEC AT 10 M
 MODEL FENCE HEIGHT = 2.0 CM
 PROTOTYPE FENCE HEIGHT = 5.0 M



CONTR. FR. 2M 1.0000 TO 15.0000 CONTR. INTERVAL OF 2.0000 PT(3,3)= .10430E-02

Figure 26. Ground-level Mean Concentration Isopleths for Run Number 20

RUN NUMBER = 26 CONFIGURATION = 1

MODEL FLOW RATE = 8946.0 CC/MIN
PROTOTYPE FLOW RATE = 40.0 (M)(M)(M)/MIN
MODEL VELOCITY = .42 M/SEC AT 4 CM
PROTOTYPE VELOCITY = 7.0 M/SEC AT 10 M
MODEL FENCE HEIGHT = 2.0 CM
PROTOTYPE FENCE HEIGHT = 5.0 M

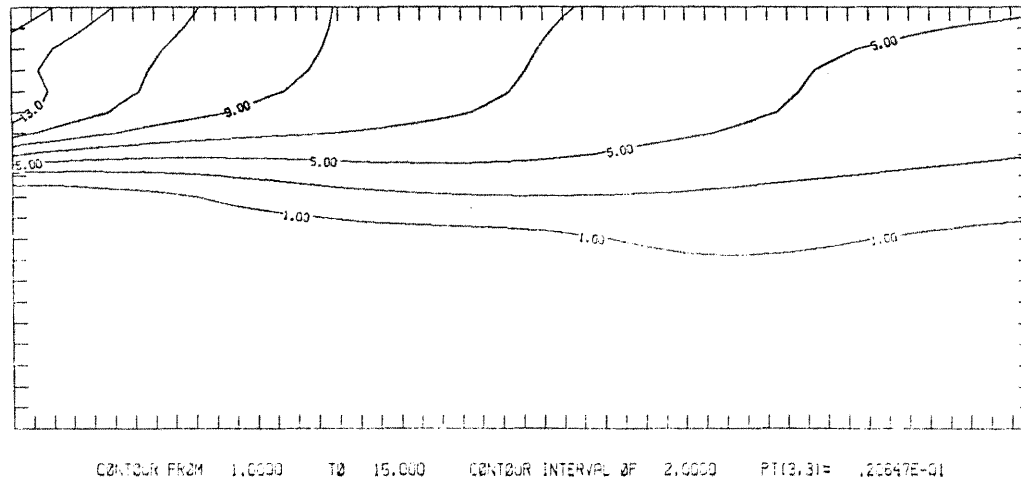
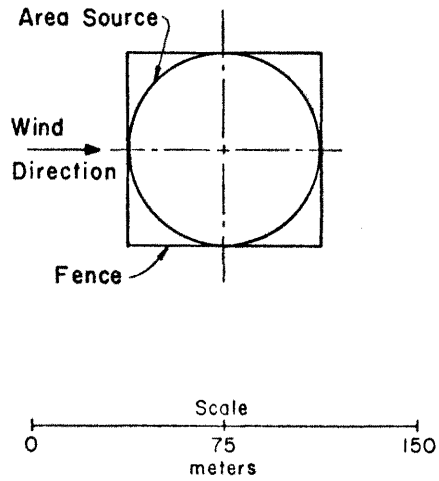
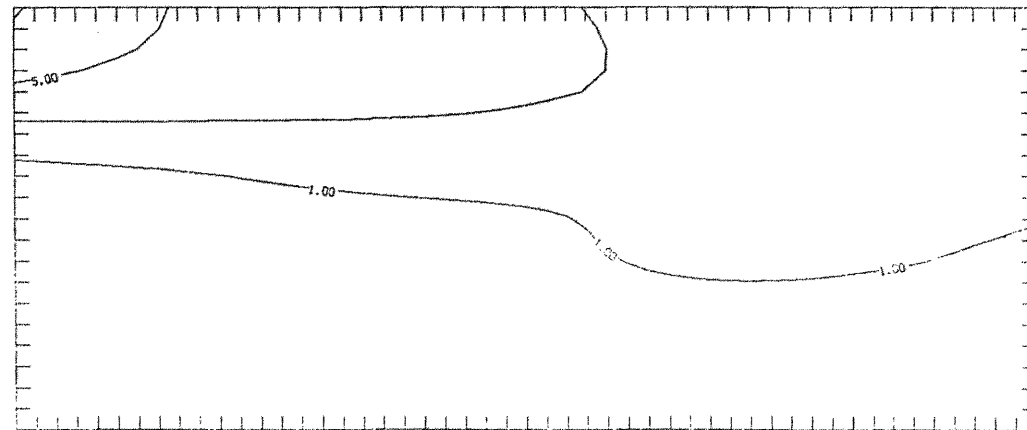
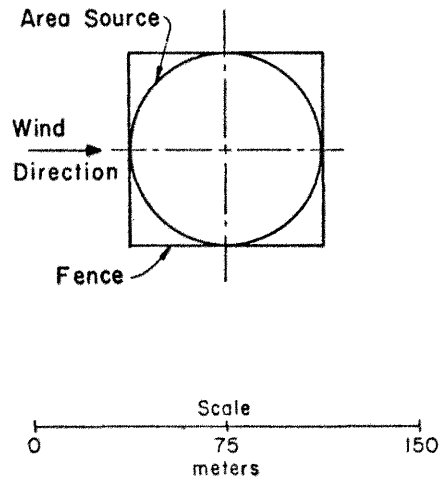


Figure 27. Ground-level Mean Concentration Isopleths for Run Number 26

RUN NUMBER = 40 CONFIGURATION = 1

MODEL FLOW RATE = 6710.0 CC/MIN
PROTOTYPE FLOW RATE = 30.0 (M)(M)(M)/MIN
MODEL VELOCITY = .52 M/SEC AT 4 CM
PROTOTYPE VELOCITY = 9.0 M/SEC AT 10 M
MODEL FENCE HEIGHT = 2.0 CM
PROTOTYPE FENCE HEIGHT = 5.0 M



CONTOUR FROM 1.0000 TO 15.0000 CONTOUR INTERVAL OF 2.0000 PT(3,3)= .3578EE-02

Figure 28. Ground-level Mean Concentration Isopleths for Run Number 40

RUN NUMBER = 58 CONFIGURATION = 1

MODEL FLOW RATE = 6710.0 CC/MIN
PROTOTYPE FLOW RATE = 30.0 (M)(M)(M)/MIN
MODEL VELOCITY = .72 M/SEC AT 4 CM
PROTOTYPE VELOCITY = 12.0 M/SEC AT 10 M
MODEL FENCE HEIGHT = 2.0 CM
PROTOTYPE FENCE HEIGHT = 5.0 M

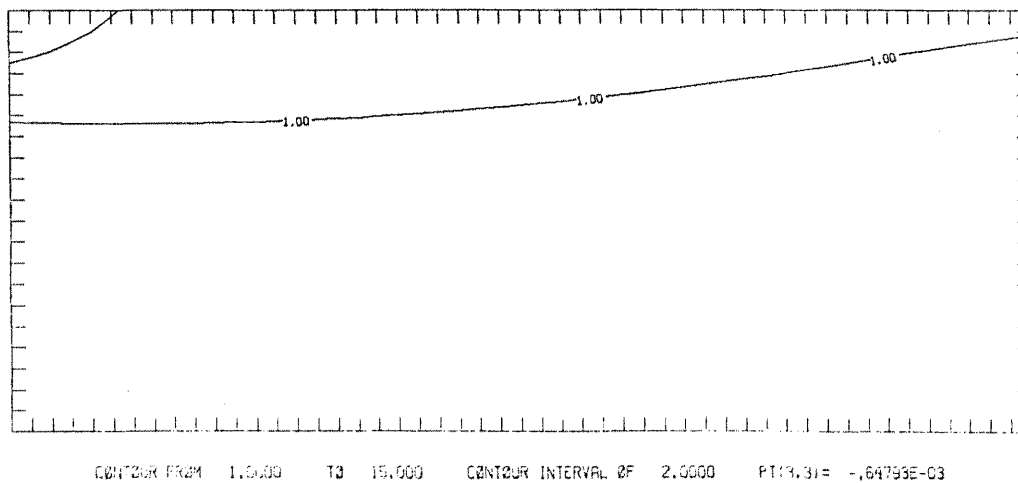
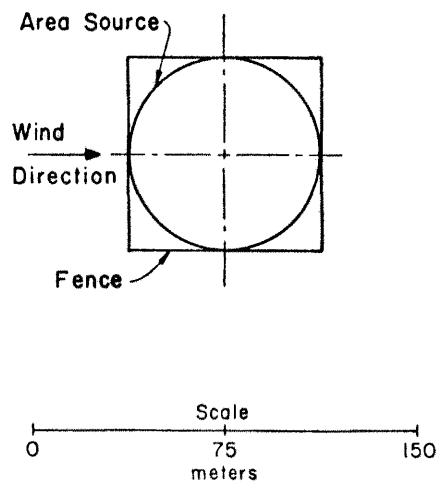


Figure 29. Ground-level Mean Concentration Isopleths for Run Number 58

RUN NUMBER = 74 CONFIGURATION = 0

MODEL FLOW RATE = 6710.0 CC/MIN
PROTOTYPE FLOW RATE = 30.0 (M)(M)(M)/MIN
MODEL VELOCITY = .24 M/SEC AT 4 CM
PROTOTYPE VELOCITY = 4.0 M/SEC AT 10 M
MODEL FENCE HEIGHT = 0.0 CM
PROTOTYPE FENCE HEIGHT = 0.0 M

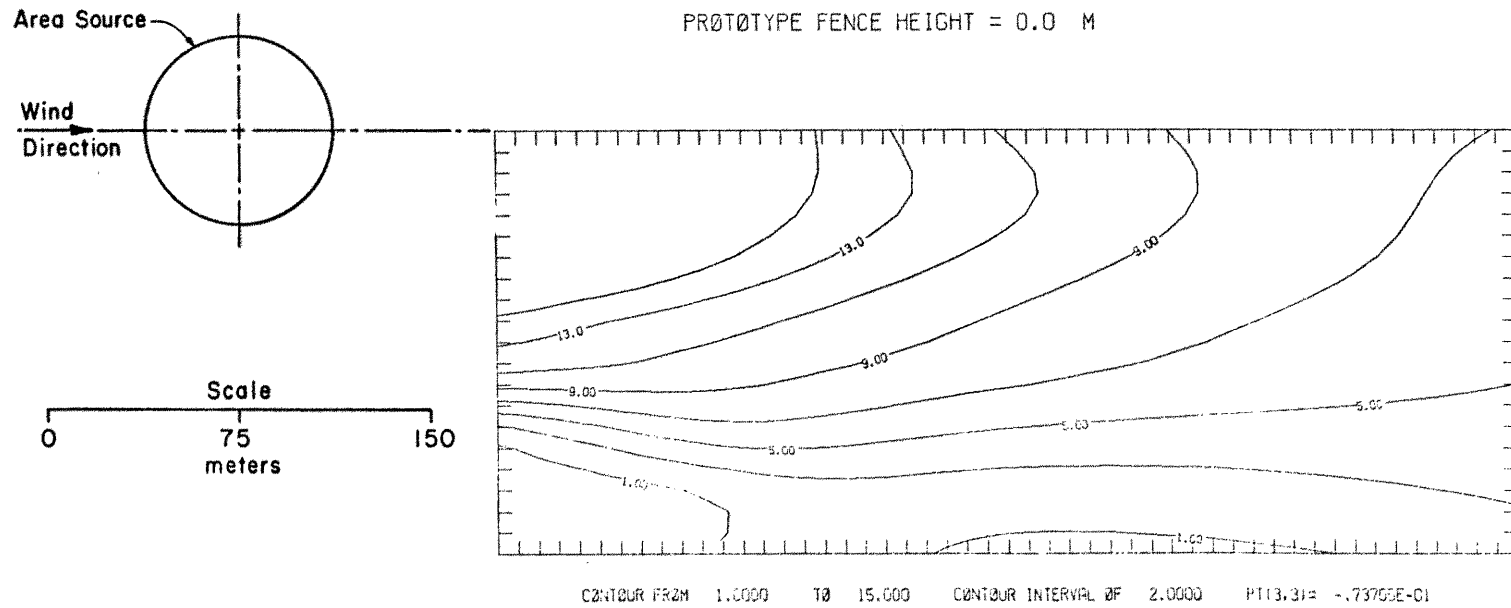
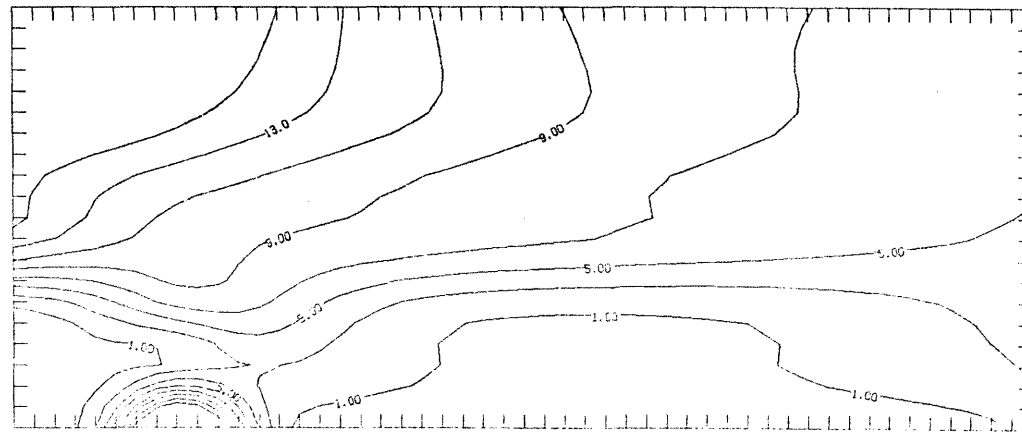
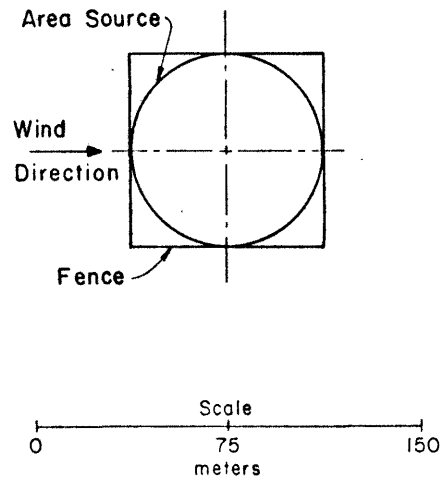


Figure 30. Ground-level Mean Concentration Isopleths for Run Number 74

RUN NUMBER = 91 CØNFIGURATIØN = 1

MØDEL FLØW RATE = 6710.0 CC/MIN
PRØTØTYPE FLØW RATE = 30.0 (M)(M)(M)/MIN
MØDEL VELOCITY = .24 M/SEC AT 4 CM
PRØTØTYPE VELOCITY = 4.0 M/SEC AT 10 M
MØDEL FENCE HEIGHT = 2.0 CM
PRØTØTYPE FENCE HEIGHT = 5.0 M

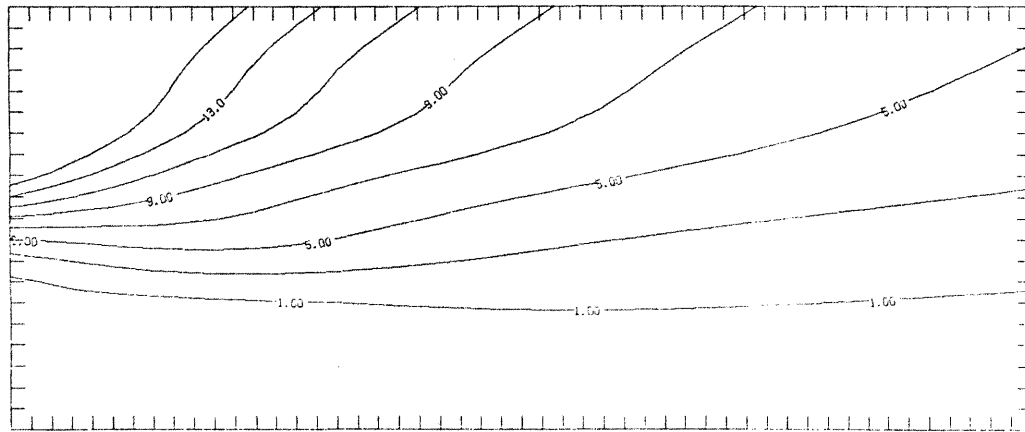
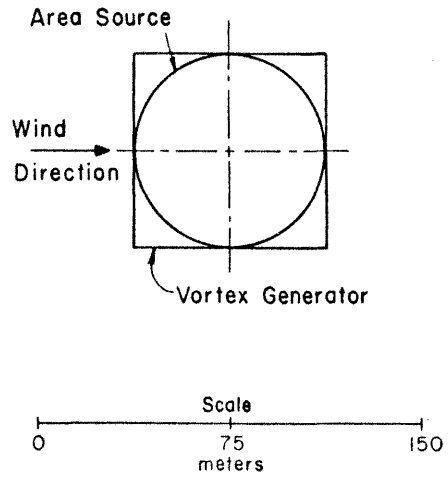


CØNTOUR FROM 1.0000 TO 15.0000 CØNTOUR INTERVAL OF 2.0000 P113.31= .22181

Figure 31. Ground-level Mean Concentration Isopleths for Run Number 91

RUN NUMBER =154 CØNFIGURATIØN =4

MØDEL FLØW RATE =6710.0 CC/MIN
PRØTØTYPE FLØW RATE =30.0 (M)(M)(M)/MIN
MØDEL VELØCITY = .24 M/SEC AT 4 CM
PRØTØTYPE VELØCITY = 4.0 M/SEC AT 10 M
MØDEL VØRTEX HEIGHT =2.0 CM
PRØTØTYPE VØRTEX HEIGHT = 5.0 M

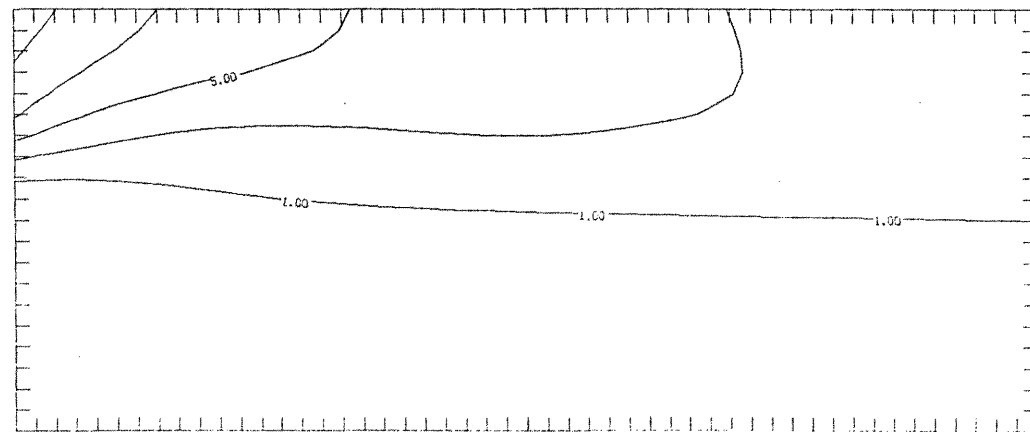
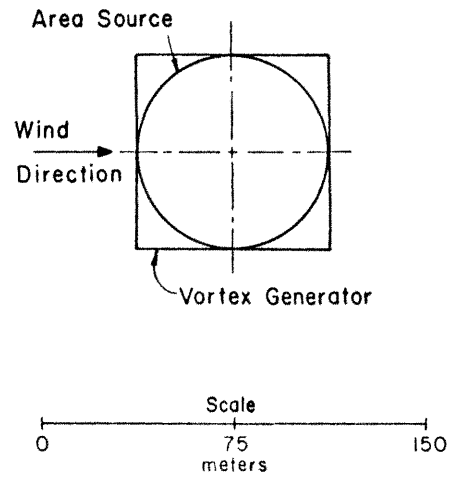


CØNTØUR FRØM 1.0000 TØ 15.0000 CØNTØUR INTERVAL ØF 2.0000 PTF(3,31)= .51778E-01

Figure 32. Ground-level Mean Concentration Isopleths for Run Number 154

RUN NUMBER =169 CONFIGURATION =4

MODEL FLOW RATE =4473.0 CC/MIN
PROTOTYPE FLOW RATE =20.0 (M)(M)(M)/MIN
MODEL VELOCITY = .42 M/SEC AT 4 CM
PROTOTYPE VELOCITY = 7.0 M/SEC AT 10 M
MODEL VORTEX HEIGHT =2.0 CM
PROTOTYPE VORTEX HEIGHT = 5.0 M



CONTOUR FROM 1.0000 TO 15.0000 CONTOUR INTERVAL OF 2.0000 PLOT SCALE .81097E-02

Figure 33. Ground-level Mean Concentration Isopleths for Run Number 169

RUN NUMBER =172 CONFIGURATION =4

MODEL FLOW RATE =6710.0 CC/MIN
PROTOTYPE FLOW RATE =30.0 (M)(M)(M)/MIN
MODEL VELOCITY = .42 M/SEC AT 4 CM
PROTOTYPE VELOCITY = 7.0 M/SEC AT 10 M
MODEL VORTEX HEIGHT =2.0 CM
PROTOTYPE VORTEX HEIGHT = 5.0 M

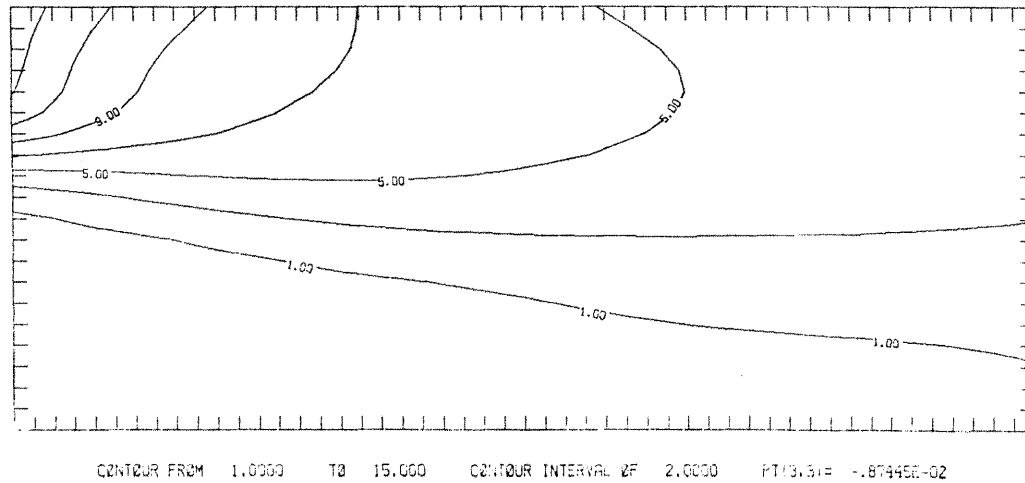
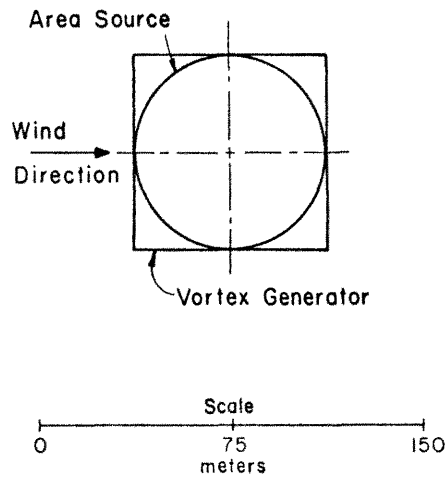
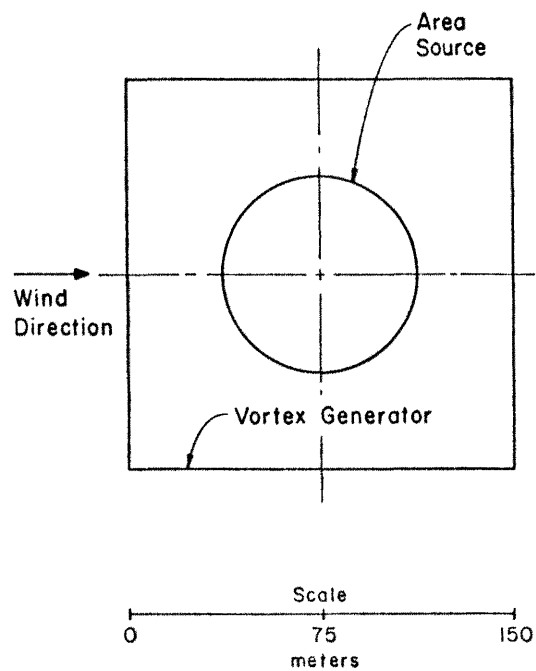
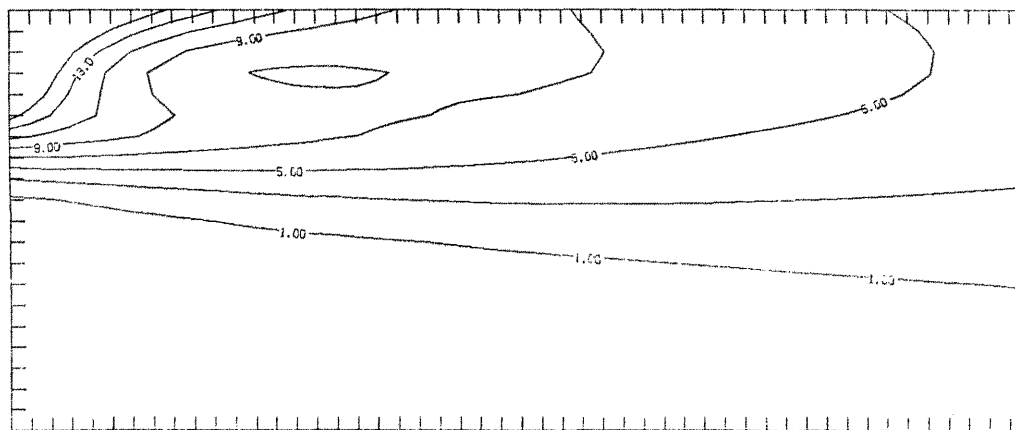


Figure 34. Ground-level Mean Concentration Isopleths for Run Number 172



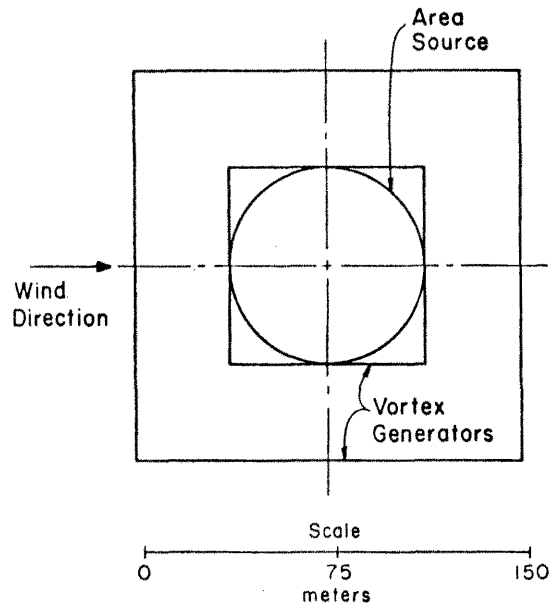
RUN NUMBER =173 CONFIGURATION =5

MODEL FLOW RATE =6710.0 CC/MIN
 PROTOTYPE FLOW RATE =30.0 (M)(M)(M)/MIN
 MODEL VELOCITY = .42 M/SEC AT 4 CM
 PROTOTYPE VELOCITY = 7.0 M/SEC AT 10 M
 MODEL VORTEX HEIGHT =2.0 CM
 PROTOTYPE VORTEX HEIGHT = 5.0 M



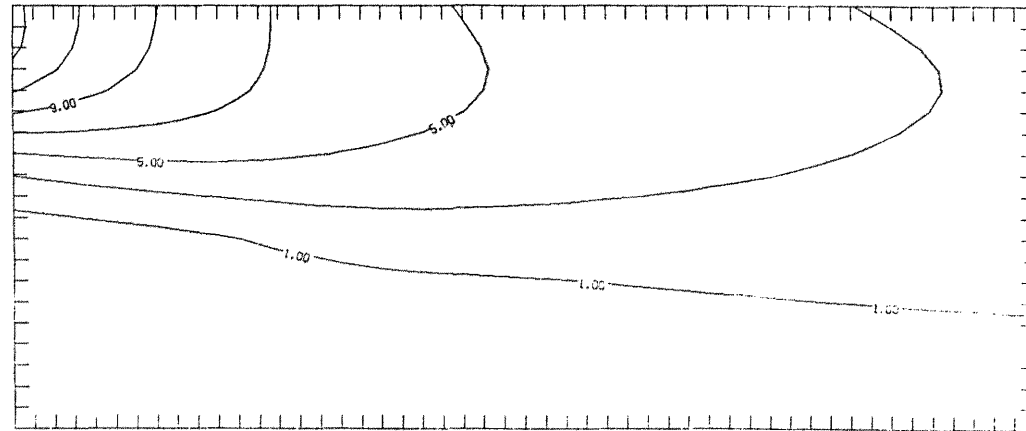
CONTOUR FROM 1.0000 TO 15.0000 CONTOUR INTERVAL OF 2.0000 PT(3,3)= .24000E-01

Figure 35. Ground-level Mean Concentration Isopleths for Run Number 173



RUN NUMBER =174 CONFIGURATION =6

MØDEL FLØW RATE =6710.0 CC/MIN
 PRØTØTYPE FLØW RATE =30.0 (M)(M)(M)/MIN
 MØDEL VELØCITY = .42 M/SEC AT 4 CM
 PRØTØTYPE VELØCITY = 7.0 M/SEC AT 10 M
 MØDEL VØRTEX HEIGHT =2.0 CM
 PRØTØTYPE VØRTEX HEIGHT = 5.0 M

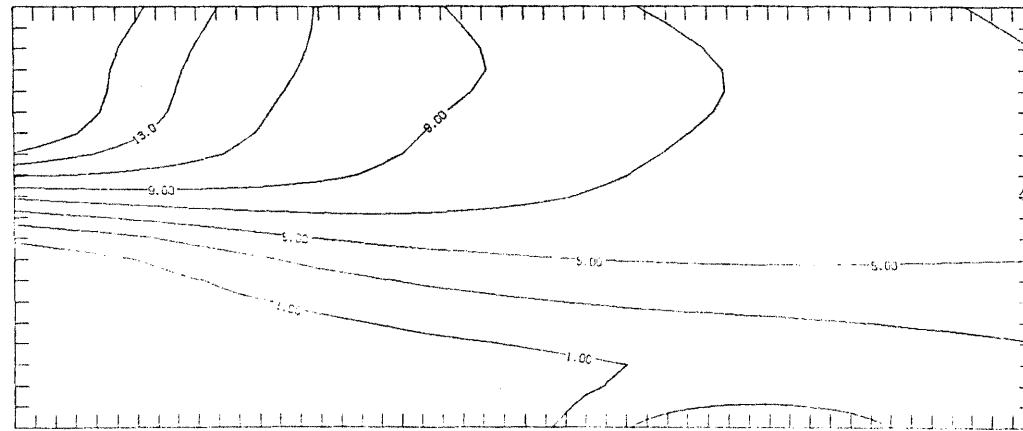
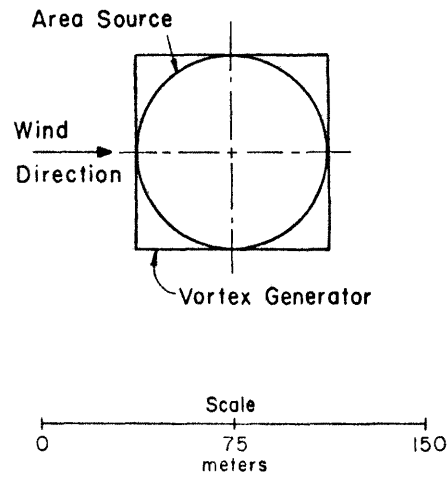


CØNTØUR FRØM 1.0000 TØ 15.000 CØNTØUR INTERVAL ØF 2.0000 P113.31= -.12710E-01

Figure 36. Ground-level Mean Concentration Isopleths for Run Number 174

RUN NUMBER =175 CONFIGURATION =4

MODEL FLOW RATE =8946.0 CC/MIN
PROTOTYPE FLOW RATE =40.0 (M)(M)(M)/MIN
MODEL VELOCITY = .42 M/SEC AT 4 CM
PROTOTYPE VELOCITY = 7.0 M/SEC AT 10 M
MODEL VORTEX HEIGHT =2.0 CM
PROTOTYPE VORTEX HEIGHT = 5.0 M

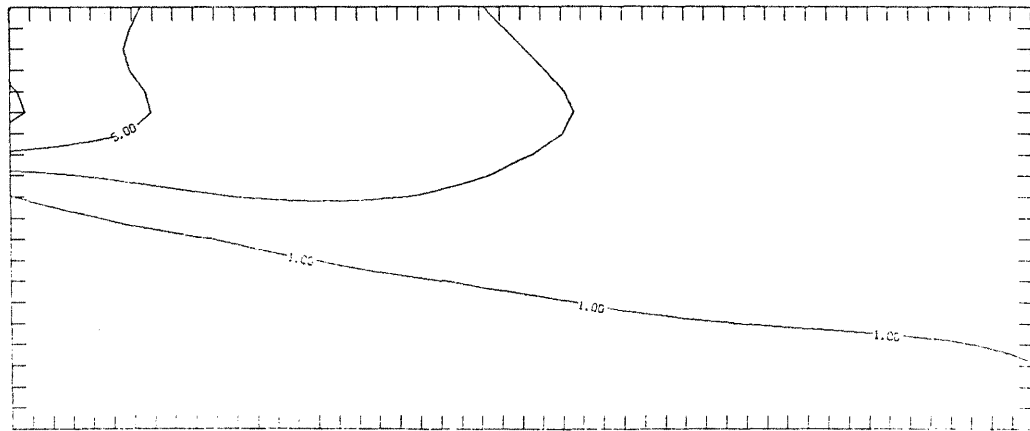
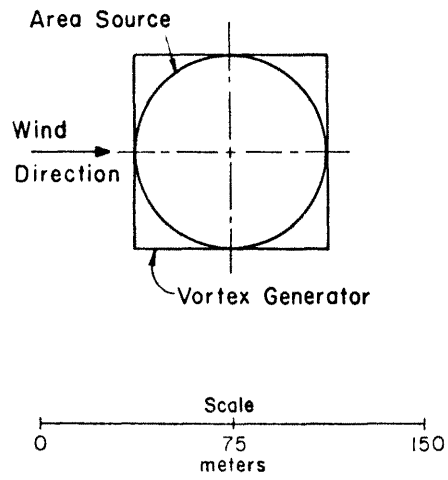


CONTOUR FROM 1.0000 TO 15.0000 CONTOUR INTERVAL OF 2.0000 P113.31E -1.35597E-01

Figure 37. Ground-level Mean Concentration Isopleths for Run Number 175

RUN NUMBER = 181 CONFIGURATION = 4

MODEL FLOW RATE = 6710.0 CC/MIN
PROTOTYPE FLOW RATE = 30.0 (M)(M)(M)/MIN
MODEL VELOCITY = .42 M/SEC AT 4 CM
PROTOTYPE VELOCITY = 7.0 M/SEC AT 10 M
MODEL VORTEX HEIGHT = 4.0 CM
PROTOTYPE VORTEX HEIGHT = 10.0 M

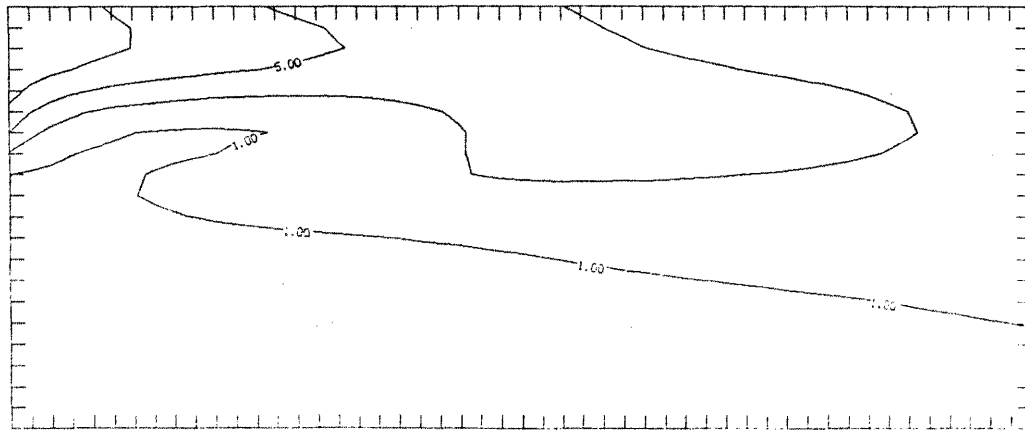
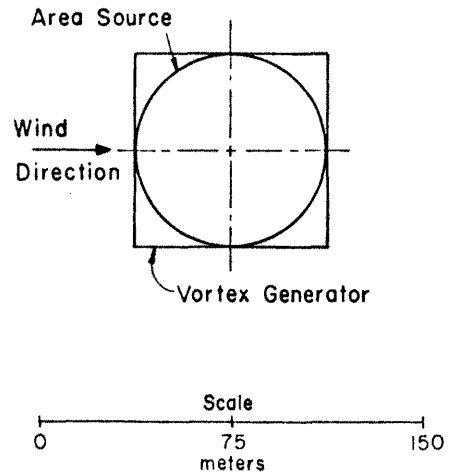


CNTR FROM 1.0000 TO 15.000 CNTR INTERVAL OF 2.0000 PLOT(S) = -1.51487E-02

Figure 38. Ground-level Mean Concentration Isopleths for Run Number 181

RUN NUMBER =190 CØNFIGURATION =4

MØDEL FLØW RATE =6710.0 CC/MIN
PRØTØTYPE FLØW RATE =30.0 (M)(M)(M)/MIN
MØDEL VELOCITY = .52 M/SEC AT 4 CM
PRØTØTYPE VELOCITY = 9.0 M/SEC AT 10 M
MØDEL VØRTEX HEIGHT =2.0 CM
PRØTØTYPE VØRTEX HEIGHT = 5.0 M



CØNTOUR FROM 1.0000 TO 15.0000 CØNTOUR INTERVAL OF 2.0000 FT(3.31) = .6620FE-03

Figure 39. Ground-level Mean Concentration Isopleths for Run Number 190

configurations, wind speeds, LNG boiloff rates, both diluting augmented devices (fences and vortex generators), and augmenting devices heights. It should be noted that Figures 17 through 21 (configuration 0) are the test runs for dispersion of LNG plume without any obstruction and are used for comparison with the fence or vortex generator runs. Table 3 to 10 present summary of all the tests performed. A complete set of data is given by Kothari et al. [27] and is available from Colorado State University or Gas Research Institute.

Figures 17 through 19 show the plots of ground-level mean concentration isopleth contours without any obstruction at LNG boiloff rates of 20, 30 and 40 m³/min at the wind speed of 7 m/sec, respectively. As expected, the ground-level concentration increases with the increase in the LNG boiloff rate. Figures 30, 18, 20 and 21 show the LNG plume dispersion at the wind speed of 4, 7, 9 and 12 m/sec, respectively, with boiloff rate of 30 m³/min. It should be noted that LNG plume gets wider as the wind speed decreases. The distance to 5% mean concentration is maximum at 7 m/sec and not at 4 m/sec. However, the distance to 5% mean concentration was reduced by increase in the wind speed from 7 m/sec.

Figures 22, 24 and 27 show the plots of ground-level mean concentration isopleth contours at LNG boiloff rates of 20, 30, 40 m³/min at the wind speed of 7 m/sec, respectively, for configuration 1 and fence height of 5 m. Similar comparison of increase in the boiloff rates at the constant wind speed for vortex generator of 5 m height are displayed in Figures 33, 34 and 37. As expected, with the increase in boiloff rates, mean concentration downwind of the sources increases. The dilution factor, defined as concentration with fence or vortex generator divided by concentration without fence or vortex generator,

Table 3. Summary of Plane Area Source

Run No.	Wind Speed m/sec	LNG Boiloff Rate m ³ /min	Maximum Mean Prototype Concentration at				Maximum Longitudinal distance to Prototype Mean Concentration of	
			100 m %	200 m %	300 m %	500 m %	9% (m)	5% (m)
73	4	20	23.7	12.8	8.3	4.9	279	492
74	4	30	30.4	17.1	11.5	6.9	374	>500
75	4	40	34.5	20.5	13.5	8.4	457	>500
1	7	20	26.4	15.8	10.3	6.0	343	>500
2	7	30	30.8	17.5	12.3	7.3	398	>500
3	7	40	35.7	20.9	14.4	9.2	>500	>500
4	9	20	24.1	12.8	8.5	5.1	285	500
5	9	30	29.4	16.8	11.5	6.6	375	>500
6	9	40	33.8	19.6	11.3	--	--	>500
7	12	20	13.7	6.0	3.2	1.6	154	235
8	12	30	22.2	11.2	6.5	2.9	246	360
9	12	40	30.5	17.6	11.4	5.4	354	>500

Table 4. Summary of Fence Data at the Wind Speed of 4 m/sec

Run No.	LNG Boiloff Rate (m ³ /min)	Fence Height (m)	Configuration Number	Maximum Mean Concentration with Fence at				Maximum Longitudinal Distance to Prototype Mean Concentration of	
				Maximum Mean Concentration without Fence	100 m	200 m	300 m	500 m	9% (m)
76	20	5	1	0.87	0.82	0.80	0.84	228	391
77	20	5	2	0.79	0.80	0.87	0.92	230	433
78	20	5	3	0.84	0.79	0.83	0.90	224	422
88	20	10	1	0.47	0.52	0.55	0.57	143	280
89	20	10	2	0.21	0.20	0.23	0.22	<100	<100
90	20	10	3	0.41	0.30	0.34	0.39	107	165
91	30	5	1	0.92	0.90	0.85	0.87	326	>500
92	30	5	2	0.63	0.57	0.63	0.68	230	457
93	30	5	3	0.79	0.75	0.73	0.78	278	470
79	30	10	1	0.60	0.60	0.59	0.64	235	404
80	30	10	2	0.32	0.28	0.31	0.33	109	191
81	30	10	3	0.47	0.35	0.37	0.43	143	237
82	40	5	1	0.98	0.96	0.96	0.96	435	>500
83	40	5	2	0.79	0.79	0.83	0.83	393	>500
84	40	5	3	0.84	0.78	0.82	0.82	370	>500
85	40	10	1	0.64	0.61	0.61	0.63	283	>500
86	40	10	2	0.46	0.43	0.51	0.54	196	428
87	40	10	3	0.55	0.41	0.45	0.52	187	404

Table 5. Summary of Fence Data at the Wind Speed of 7 m/sec

Run No.	LNG Boiloff Rate (m ³ /min)	Fence Height (m)	Configuration Number	Maximum Mean Concentration with Fence at				Maximum Longitudinal Distance to Prototype Mean Concentration of	
				Maximum Mean Concentration without Fence				9% (m)	5% (m)
				100 m	200 m	300 m	500 m		
10	20	5	1	0.26	0.28	0.28	0.33	<100	157
11	20	5	2	0.47	0.33	0.37	0.38	122	202
12	20	5	3	0.22	0.20	0.17	0.17	<100	124
22	20	10	1	0.16	0.18	0.21	0.27	<100	<100
23	20	10	2	0.09	0.09	0.10	0.15	<100	<100
24	20	10	3	0.12	0.12	0.11	0.05	<100	<100
18	30	5	1	0.39	0.38	0.49	0.47	137	287
19	30	5	2	0.52	0.37	0.38	0.48	148	280
20	30	5	3	0.32	0.29	0.25	0.25	122	202
14	30	10	1	0.20	0.22	0.24	0.30	<100	130
15	30	10	2	0.09	0.12	0.14	0.16	<100	<100
16	30	10	3	0.15	0.15	0.13	0.08	<100	<100
26	40	5	1	0.47	0.47	0.51	0.57	226	>500
27	40	5	2	0.56	0.40	0.46	0.49	185	440
28	40	5	3	0.49	0.45	0.46	0.40	209	387
30	40	10	1	0.24	0.27	0.31	0.31	<100	250
31	40	10	2	0.11	0.12	0.13	0.15	<100	<100
32	40	10	3	0.23	0.20	0.18	0.17	<100	172

Table 6. Summary of Fence Data at the Wind Speed of 9 m/sec

Run No.	LNG Boiloff Rate (m ³ /min)	Fence Height (m)	Configuration Number	Maximum Mean Concentration with Fence				at	Maximum Longitudinal Distance to Prototype	
				Maximum Mean Concentration without Fence					Mean Concentration of 9%	5%
				100 m	200 m	300 m	500 m	(m)	(m)	
34	20	5	1	0.15	0.18	0.19	0.22	<100	<100	
35	20	5	2	0.35	0.28	0.31	0.33	<100	140	
36	20	5	3	0.14	0.16	0.15	0.18	<100	<100	
37	20	10	1	0.11	0.13	0.16	0.20	<100	<100	
38	20	10	2	0.06	0.09	0.11	0.14	<100	<100	
39	20	10	3	0.08	0.09	0.12	0.12	<100	<100	
40	30	5	1	0.24	0.25	0.28	0.33	<100	150	
41	30	5	2	0.27	0.18	0.15	0.12	<100	155	
42	30	5	3	0.20	0.21	0.20	0.24	<100	126	
43	30	10	1	0.11	0.13	0.13	0.15	<100	<100	
44	30	10	2	0.07	0.08	0.10	0.15	<100	<100	
45	30	10	3	0.08	0.10	0.10	0.12	<100	<100	
46	40	5	1	0.25	0.23	0.29	--	<100	174	
47	40	5	2	0.33	0.24	0.32	--	137	210	
48	40	5	3	0.30	0.30	0.34	--	115	220	
49	40	10	1	0.13	0.14	0.19	--	<100	<100	
50	40	10	2	0.09	0.11	0.14	--	<100	<100	
51	40	10	3	0.12	0.13	0.16	--	<100	<100	

Table 7. Summary of Fence Data at the Wind Speed of 12 m/sec

Run No.	LNG Boiloff Rate (m ³ /min)	Fence Height (m)	Configuration Number	Maximum Mean Concentration with Fence at				Maximum Longitudinal Distance to Prototype Mean Concentration of	
				Maximum Mean Concentration without Fence				9% (m)	5% (m)
				100 m	200 m	300 m	500 m		
52	20	5	1	0.20	0.25	0.34	0.50	<100	<100
53	20	5	2	0.34	0.32	0.50	0.63	<100	<100
54	20	5	3	0.18	0.25	0.31	0.44	<100	<100
55	20	10	1	0.12	0.13	0.19	0.19	<100	<100
56	20	10	2	0.08	0.12	0.16	0.19	<100	<100
57	20	10	3	0.09	0.12	0.19	0.25	<100	<100
58	30	5	1	0.19	0.20	0.25	0.38	<100	<100
59	30	5	2	0.27	0.23	0.31	0.45	<100	113
60	30	5	3	0.17	0.20	0.23	0.34	<100	<100
61	30	10	1	0.12	0.15	0.20	0.31	<100	<100
62	30	10	2	0.08	0.10	0.14	0.24	<100	<100
63	30	10	3	0.08	0.12	0.14	0.24	<100	<100
64	40	5	1	0.17	0.20	0.22	0.31	<100	109
65	40	5	2	0.29	0.20	0.24	0.33	<100	150
66	40	5	3	0.18	0.19	0.18	0.28	<100	110
67	40	10	1	0.12	0.11	0.15	0.24	<100	<100
68	40	10	2	0.07	0.09	0.11	0.19	<100	<100
69	40	10	3	0.08	0.09	0.11	0.19	<100	<100

Table 8. Vortex Generator Data at the Wind Speed of 4 m/sec

Run No.	LNG Boiloff Rate (m ³ /min)	V.G. Height (m)	Configuration Number	Maximum Mean Concentration with V.G. at				Maximum Longitudinal Distance to Prototype Mean Concentration of	
				Maximum Mean Concentration without V.G.				9% (m)	5% (m)
				100 m	200 m	300 m	500 m		
151	20	5	4	0.85	0.77	0.76	0.69	217	365
152	20	5	5	1.04	0.87	0.86	0.86	241	421
153	20	5	6	0.82	0.70	0.67	0.59	200	330
160	20	10	4	0.49	0.45	0.45	0.41	128	228
161	20	10	5	0.89	0.36	0.34	0.27	141	191
162	20	10	6	0.50	0.35	0.36	0.33	120	184
154	30	5	4	0.95	0.85	0.83	0.77	314	>500
155	30	5	5	1.05	0.91	0.95	0.91	363	>500
156	30	5	6	0.99	0.82	0.78	0.77	298	>500
163	30	10	4	0.70	0.60	0.57	0.54	226	385
164	30	10	5	0.99	0.48	0.49	0.42	187	330
165	30	10	6	0.71	0.49	0.48	0.49	188	337
157	40	5	4	0.96	0.81	0.81	0.70	354	>500
158	40	5	5	1.05	0.89	0.93	0.88	417	>500
159	40	5	6	0.96	0.75	0.77	0.61	341	>500
166	40	10	4	0.84	0.67	0.67	0.63	304	>500
167	40	10	5	1.08	0.61	0.61	0.58	290	>500
168	40	10	6	0.87	0.60	0.63	0.63	280	>500

Table 9. Vortex Generator Data at the Wind Speed of 7 m/sec

Run No.	LNG Boiloff Rate (m ³ /min)	V.G. Height (m)	Configuration Number	Maximum Mean Concentration with V.G. at				Maximum Longitudinal Distance to Prototype Mean Concentration of	
				Maximum Mean Concentration without V.G.				9% (m)	5% (m)
				100 m	200 m	300 m	500 m		
169	20	5	4	0.39	0.39	0.38	0.37	116	233
170	20	5	5	0.65	0.39	0.29	0.22	150	225
171	20	5	6	0.31	0.28	0.28	0.30	<100	166
178	20	10	4	0.14	0.15	0.17	0.20	<100	<100
179	20	10	5	0.65	0.30	0.28	0.28	135	184
180	20	10	6	0.22	0.19	0.19	0.20	<100	117
172	30	5	4	0.47	0.46	0.49	0.48	176	361
173	30	5	5	0.92	0.66	0.61	0.62	250	461
174	30	5	6	0.44	0.40	0.39	0.37	157	285
181	30	10	4	0.23	0.23	0.25	0.30	<100	157
182	30	10	5	0.82	0.36	0.32	0.33	163	239
183	30	10	6	0.29	0.23	0.22	0.23	<100	163
175	40	5	4	0.58	0.57	0.60	0.59	285	>500
176	40	5	5	0.97	0.72	0.69	0.65	341	>500
177	40	5	6	0.57	0.52	0.53	0.49	252	457
184	40	10	4	0.24	0.22	0.27	0.28	107	220
185	40	10	5	0.86	0.37	0.34	0.33	185	293
186	40	10	6	0.33	0.26	0.26	0.26	133	222

Table 10. Vortex Generator Data at the Wind Speed of 9 m/sec

Run No.	LNG Boiloff Rate (m ³ /min)	V.G. Height (m)	Configuration Number	Maximum Mean Concentration with V.G.				at	Maximum Longitudinal Distance to Prototype	
				Maximum Mean Concentration without V.G.					9% Mean Concentration of	5% Mean Concentration of
				100 m	200 m	300 m	500 m	(m)	(m)	
187	20	5	4	0.23	0.25	0.28	0.29	<100	122	
188	20	5	5	0.46	0.29	0.24	0.18	115	164	
189	20	5	6	0.24	0.26	0.28	0.29	<100	122	
196	20	10	4	0.13	0.15	0.18	0.22	<100	<100	
197	20	10	5	0.41	0.23	0.22	0.24	105	143	
198	20	10	6	0.14	0.14	0.15	0.18	<100	<100	
190	30	5	4	0.30	0.30	0.33	0.38	<100	230	
191	30	5	5	0.69	0.47	0.40	0.41	182	283	
192	30	5	6	0.29	0.27	0.29	0.32	<100	185	
199	30	10	4	0.16	0.17	0.20	0.24	<100	<100	
200	30	10	5	0.60	0.28	0.30	0.33	138	191	
201	30	10	6	0.19	0.17	0.18	0.21	<100	114	
193	40	5	4	0.38	0.37	0.41	--	157	354	
194	40	5	5	0.75	0.51	0.54	--	216	357	
195	40	5	6	0.36	0.35	0.42	--	146	287	
202	40	10	4	0.20	0.20	0.28	--	<100	159	
203	40	10	5	0.74	0.35	0.42	--	167	265	
204	40	10	6	0.24	0.20	0.27	--	<100	159	

increases with increase in boiloff rate under identical wind speed. This indicates that with higher LNG boiloff rate the plume is much more stable and turbulence induced by the fences or vortex generators is less effective for mixing of the plume. Figures 31, 24, 28 and 29 show the mean concentration isopleths for the LNG boiloff rate of $30 \text{ m}^3/\text{min}$, fence of 5 m height and configuration 1 for the wind speed of 4, 7, 9 and 12 m/sec, respectively. The similar comparison is given in Figures 32, 34 and 39 for vortex generator of 5 m height and configuration 4. It can be concluded that lower wind speed resulted in higher ground level concentration and corresponding longer distances to LFL when the surface obstacle (fence or vortex generator) interacts with the LNG plume. However, for the unobstructed case, the intermediate wind speed (7 m/sec) gave the maximum concentration. Similar conclusions were drawn by Kothari et al. [5] from experiments of LNG plume interaction with surface obstacles.

Figures 18, 24, 25, 26, 34, 35 and 36 show the mean ground-level concentration isopleths at wind speed of 7 m/sec, LNG boiloff rate of $30 \text{ m}^3/\text{min}$, for configurations 0, 1, 2, 3, 4, 5 and 6, respectively. The measured concentrations were always smaller in magnitude with a fence or vortex generator than without any obstruction case. The fence or vortex generator creates higher turbulence intensity and hence larger spread of LNG plume and quicker plume dilution. Similar, higher turbulence intensity in the wake of surface obstacles was observed by Kothari et al. [28], Woo et al. [29], Hansen et al. [30], Castro and Robins [31], and Counihan [32]. Generally, the concentrations measured with double fences or double vortex generators (configuration 3 or 6) were smaller in magnitude than with single fences or vortex generators. However, the

difference in concentration between configurations 1 and 3 or 4 and 6 was small and would probably not justify the additional fence or vortex generator downwind. It was also noted that the concentrations were slightly higher for configuration 2 or 5 as compared with configuration 1 or 4 for all cases except for fence data at 4 m/sec wind speed. This indicates that the maximum dilution can be obtained when the augmenting devices such as fences or vortex generators were closest to the area source generating LNG plume. Similar findings were observed by Kothari et al. [5] for other surface obstacles.

Figures 24, 23, 34 and 38 represent the ground level mean concentration isopleths for $30 \text{ m}^3/\text{min}$ LNG boiloff rate, 7 m/sec wind speed for configurations 1, 1, 4, and 4 with the augmenting device heights of 5, 10, 5 and 10 m, respectively. As expected, the higher the heights of augmenting devices, the lower the concentrations. The vortex generator produced a vortex pair which suppressed vertical mixing and reduced the turbulence intensity. Hence, it was observed that, in general, solid fences gave the higher dilution than the vortex generators. The LNG plume tended to have its maximum concentration off the centerline for all downwind distances, especially for configuration 0. This result with no augmenting device is attributed to the plume traveling off the centerline of wind tunnel due to slight lateral nonuniformity in the flow. However, when the same phenomenon occurred with fences, it could also have been due to higher turbulence intensity in the wake of fences leading to higher entrainment and correspondingly lower concentration in the wake. The occurrence of offcenter line

maximum concentrations with vortex generators could also be related to higher turbulence intensity in the wake of the vortex generator or to the effects of a vortex pair generated by the augmenting devices.

5.0 CONCLUSIONS

The wind-tunnel test program was conducted on a 1:250 scale model to determine the effects of fences and vortex generators on the dispersion of LNG plumes. The tests were conducted to simulate continuous LNG boiloff rates of 20, 30 and 40 m³/min; four wind speeds, 4, 7, 9 and 12 m/sec at 10 m height for fence data and three wind speeds, 4, 7 and 9 m/sec at 10 m height for vortex generator data; and 7 configurations. The results led to the following conclusions:

- At the same downwind distance, the highest concentrations were observed without fences or vortex generators, i.e. fences and vortex generators enhance LNG vapor dispersion, resulting in a reduction of ground-level hazards.
- In general, a lower wind speed resulted in a higher ground-level concentration when the fences or vortex generators were present. However, for the no fence or vortex generator case, the intermediate wind speed (7 m/sec) gave highest concentration.
- As expected, the ground-level concentration at a given point was increased with increased in LNG boiloff rates.
- The dilution factor, defined as the ratio of concentration with fence or vortex generator to concentration without fence or vortex generator, is increased with the increase in boiloff rate under identical wind speed. This indicates that with higher LNG boiloff rate the plume is much more stable and turbulence induced by the fences or vortex generator is less effective for mixing of the plume.
- The ground-level concentration was reduced with increase in fence or vortex generator height, as expected.

- In general, the dilution factor was smaller with the solid fence compared with the vortex generator under identical conditions. This could be attributed to the vortex pair, generated by the vortex generator, suppressing vertical mixing.
- In general, the fence or vortex generator closer to the LNG area source produced greater LNG plume dilution than the fence or vortex generator away from the area source. This indicates that if the devices such as fences or vortex generators are used, they should be as close as possible to the LNG spill area.

REFERENCES

1. American Gas Association (1974) "LNG Safety Program, Interim Report on Phase II Work," Report on American Gas Association Project IS-3-1, Battelle Columbus Laboratories.
2. Neff, D. E., Meroney, R. N., and Cermak, J. E. (1976) "Wind Tunnel Study of Negatively Buoyant Plume Due to an LNG Spill," Report prepared for R & D Associates, California, Fluid Dynamics and Diffusion Laboratory Report CER76-77DEN-RNM-JEC22, Colorado State University, Fort Collins, Colorado, 241 p.
3. Neff, D. E. and Meroney, R. N. (1981) "The Behavior of LNG Vapor Clouds: Wind-Tunnel Simulation of 40 m³ LNG Spill Tests at China Lake Naval Weapons Center, California," Colorado State University Report CER81-82DEN-RNM1 for Gas Research Institute, GRI Report 80/0094.
4. Neff, D. E. and Meroney, R. N. (1982) "The Behavior of LNG Vapor Clouds: Wind-Tunnel Tests on the Modeling of Heavy Plume Dispersion," GRI Report 80/0145.
5. Kothari, K. M., Meroney, R. N., and Neff, D. E. (1981) "LNG Plume Interaction with Surface Obstacles," Gas Research Institute Report GRI 80/0095.
6. Hinze, J. O. (1975) Turbulence, McGraw-Hill, 790 p.
7. Pasquill, F. (1974) Atmospheric Diffusion, D. von Nostrand Co., 429 p.
8. Cermak, J. E. (1971) "Laboratory Simulation of the Atmospheric Boundary Layer," AIAA J., Vol. 9, No. 9, pp. 1746-1754, September.
9. Kline, S. J. (1965) Similitude and Approximation Theory, McGraw-Hill, 229 p.
10. Cermak, J. E. (1975) "Applications of Fluid Mechanics to Wind Engineering, A Freeman Scholar Lecture," J. of Fluid Engineering, Vol. 97, Ser. 1, No. 1, pp. 9-38.
11. Schlichting, H. (1968) Boundary Layer Theory, McGraw-Hill, New York.
12. Zoric, D. and Sandborn, V. A. (1972) "Similarity of Large Reynolds Number Boundary Layers," Boundary-Layer Meteorology, Vol. 2, No. 3, March, pp. 326-333.
13. Halitsky, J. (1969) "Validation of Scaling Procedures for Wind Tunnel Model Testing of Diffusion Near Buildings," Geophysical Sciences Laboratory, Report No. TR-69-8, New York University, New York.

14. Plate, E. J. and Cermak, J. E. (1963) "Micro-Meteorological Wind-Tunnel Facility: Description and Characteristics," Fluid Dynamics and Diffusion Laboratory Report CER63-ELP-JEC9, Colorado State University, Fort Collins, Colorado.
15. Counihan, J. (1975) "Adiabatic Atmospheric Boundary Layers: A Review and Analysis of Data from the Period 1880-1972," Atmospheric Environment, Vol. 9, pp. 871-905.
16. Hoot, T. G., et al. (1974) "Wind Tunnel Tests of Negatively Buoyant Plumes," Fluid Dynamics and Diffusion Laboratory Report CER73-74TGH-RNM-JAP-13, Colorado State University, Fort Collins, Colorado, October.
17. Skinner, G. T. and Ludwig, G. R. (1978) "Physical Modeling of Dispersion in the Atmospheric Boundary Layer," Calspan Advanced Technology Center, Calspan Report No. 201, May.
18. Snyder, W. H. (1972) "Similarity Criteria for the Application of Fluid Models to the Study of Air Pollution Meteorology," Boundary Layer Meteorology, Vol. 3, No. 1, September.
19. Boyle, G. J. and Kneebone, A. (1973) "Laboratory Investigation into the Characteristics of LNG Spills on Water, Evaporation, Spreading and Vapor Dispersion," Shell Research, Ltd., Report to API, March.
20. Meroney, R. N., Neff, D. E., Cermak, J. E., and Megahed, M. (1977) "Dispersion of Vapor from LNG Spills - Simulation in a Meteorological Wind Tunnel," Report prepared for R & D Associates, California, Fluid Dynamics and Diffusion Laboratory Report CER76-77RNM-JEC-DEN-MM57, Colorado State University, Fort Collins, Colorado, 151 p.
21. Kothari, K. M. and Meroney, R. N. (1979) "Building Effects on National Transonic Facility Exhaust Plume," A Technical Report Prepared for NASA, Hampton, Virginia, also, Colorado State University Report CER79-80KMK-RNM35.
22. Meroney, R. N., et al. (1974) "Wind Tunnel Study of Stack Gas Dispersal at the Avon Lake Power Plant," Fluid Dynamics and Diffusion Laboratory Report CER73-74RNM-JEC-BTY-SKN35, Colorado State University, Fort Collins, Colorado, April.
23. Bodurtha, F. T., Jr. (1961) "The Behavior of Dense Stack Gases," J. of APCA, Vol. 11, No. 9, pp. 431-437.
24. van Ulden, A. P. (1974) "On the Spreading of a Heavy Gas Released Near the Ground," Loss Prevention and Safety Promotion Seminar, Delft, Netherlands, 6 p.
25. Fay, J. A. (1980) "Gravitational Spread and Dilution of Heavy Vapor Clouds," Second International Symposium on Stratified Flows, the Norwegian Institute of Technology, Trondheim, Norway, 24-27 June.

26. Sandborn, V. A. (1972) Resistance Temperature Transducers, Metrology Press, 545 p.
27. Kothari, K. M. and Meroney, R. N. (1982) "Accelerated Dilution of Liquefied Natural Gas Plumes with Fences and Vortex Generators: Data Tables," A technical report submitted to Gas Research Institute.
28. Kothari, K. M., Peterka, J. A., and Meroney, R. N. (1979) "Stably Stratified Building Wakes," U.S. Nuclear Regulatory Commission Report NUREG/CR-1247.
29. Woo, H. G. C., Peterka, J. A., and Cermak, J. E. (1976) "Wind Tunnel Measurements in the Wakes of Structures," Colorado State University Report CER75-76-HGCW-JAP-JEC40, Colorado State University, Fort Collins, Colorado.
30. Hansen, A. C. and Cermak, J. E. (1975) "Vortex-Containing Wakes of Surface Obstacles," Colorado State University Report CER75-76ACH-JEC16, Colorado State University, Fort Collins, Colorado.
31. Castro, J. P., and Robins, A. G. (1975) "The Effect of a Thick Incident Boundary Layer on the Flow Around a Small Surface Mounted Cube," Central Electricity Generating Board Report R/M/N795, England.
32. Counihan, J. (1971) "An Experimental Investigation of the Cube behind a Two-Dimensional Block and behind a Cube in a Simulated Boundary Layer Flow," Centered Electricity Generating Board Report RD/L/N115/71.

APPENDIX A
THE CALCULATION OF MODEL SCALE FACTORS

APPENDIX A - THE CALCULATION OF MODEL SCALE FACTORS

As discussed previously in Section 2.3 the dominant scaling criteria for the simulation of LNG vapor cloud physics are the Froude number and the volume flux ratio. By setting these parameters equal for model and prototype one obtains the following relationships.

$$(U_a)_m = \left(\frac{S.G._m - 1}{S.G._p - 1} \right)^{1/2} \left(\frac{1}{L.S.} \right)^{1/2} (U_a)_p$$

$$Q_m = \left(\frac{S.G._m - 1}{S.G._p - 1} \right)^{1/2} \left(\frac{1}{L.S.} \right)^{5/2} Q_p$$

$$L_m = \left(\frac{1}{L.S.} \right) L_p$$

In addition to these scaling parameters which govern the flow physics, one must also scale the mole fractions (concentrations) measured in the model to those that would occur in the prototype. This scaling is required since the number of moles being released in a thermal plume are different from the number of moles being released in a isothermal plume. To be more precise the relationship between the molar flow rate of source gas in the model and the prototype is

$$n_p = \left(\frac{T_m}{T_p} \right)_{@ \text{ b.o.}} n_m = (2.70) n_m$$

By definition the concentration of LNG vapor is expressed as:

$$\chi_p = n_{NG} / (n_{NG} + n_a)$$

Substituting model equivalents into the above expression yields

$$\chi_p = \frac{\left(\frac{T_m}{T_p} \right)_{@ \text{ b.o.}} n_{Ar}}{\left(\frac{T_m}{T_p} \right)_{@ \text{ b.o.}} n_{Ar} + n_a} = \frac{n_{Ar}}{n_{Ar} + n_a \left(\frac{T_p}{T_m} \right)_{@ \text{ b.o.}}}$$

or

$$x_p = \frac{x_m}{x_m + (1 - x_m)(0.37)}$$

This equation was used to correct the modeled measurements to those that would be observed in the field.